PREDICTION OF FINITE SPAN HYDROFOIL CHARACTERISTICS AT SHALLOW SUBMERGENCES USING IMAGE STABILIZING CRITERION.

BY

DEBBRATA PAUL

A thesis submitted to the Department of Mechanical Engineering in Partial fulfilment of the requirements for the degree of Master of Science in Mechanical Engineering.

February, 1989

BANGLADESH UNIVERSITY OF ENGINEERING AND TECHNOLOGY,

DHAKA, BANGLADESH

RECOMMENDATION OF THE BOARD OF EXAMINERS

The Board of Examiners hereby recommends to the Department of Mechanical Engineering, BUET, Dhaka, acceptance of the thesis "PREDICTION OF FINITE SPAN HYDROFOIL CHARACTERISTICS AT SHALLOW SUBMERGENCES USING IMAGE STABILIZING CRITERION", Submitted by Debbrata Paul, in partial fulfilment of the requirements for the degree of Master of Sceince in Mechanical Engineering.

Chairman :

Dr. Md. Quamrul Islam
Associate Professor
Department of Mechanical Engineering
BUET, Dhaka.

(Co-Supervisor)

Dr. Md. Refayet Ullah
Assistant Professor
Department of Naval Architecture
and Marine Engineering
BUET, Dhaka.

Member

Dr. Dibak Kanti Das
Professor
Department of Mechanical Engineering
BUET, Dhaka.

Member

Dr. Amalesh Chandra Mandal
Professor
Department of Mechanical Engineering
BUET, Dhaka.

Member

Dr. Abul Fazal Md. Saleh
Associate Professor
Institute of Flood Control and
Drainage Research , BUET, Dhaka.

February, 1989

CERTIFICATE OF RESEARCH

This is to certify that the work presented in thesis is an outcome of the investigation carried out by the author under the supervision of Dr. Md. Quamrul Islam, Department of Mechanical Engineering and Dr. Md. Refayet Ullah, Department of Naval Architecture and Marine Engineering, B.U.E.T., Dhaka.

Supervisor	Co-supervisor	Author

Debbrata Paul

DECLARATION

This is to hereby declared that neither this thesis nor any part thereof has been submitted or is being concurrently submitted anywhere else for the award of any degree or diploma or for any publication.

Debbrata Paul

Author

ACKNOWLEDGEMENT

With deep sincerity, the author expresses his profound indebtedness to Dr.Md.Quamrul Islam, Associate Professor ,Mechanical Engineering Department and Dr.Md.Refayet Ullah,Assistant Professor, Naval Architecture and Marine Engineering Department,BUET,for their guidance, constant encouragement and invaluable suggestions in achieving every minute detail of this thesis.

The author is highly grateful to Professor Dipak Kanti Das, Professor Amalesh Chandra Mandal,Mechanical Engineering Department,BUET,for their suggestions and help.The author is also thankful to Dr. Abul Fazal Md. Saleh,Associate Professor,IFCDR,BUET,for his good advice.

The author is also indebted to Professor Mahiuddin Chowdhury, Head of the Naval Architecture and Marine Engineering Department,BUET,for providing with the microcomputer facilities of the department. Thanks are due to Mr. Abdur Rahim,Assistant Professor of the same department,BUET,for helping in microcomputer and wardstar operation.

ABSTRACT

The lift force generated by the hydrofoil elevates the craft above the water surface. So, for hydrofoil craft the prediction of foil characteristics is very important. As the foil moves beneath the water surface the free water surface is disturbed. Hence to predict the foil characteristics the free surface effect should be considered. To consider this free surface effect, it is assumed that there is a image of the hydrofoil at a distance equal to depth of submergence from the interface in the air. The total effect of body and image on the foil characteristics is the actual characteristics of the foil.

The solution procedure involves lifting line theory and vortex lattice method. In lifting line theory the hydrofoil body is considered as a line along the span located at the quarter chord mean line. In vortex lattice method the hydrofoil body is divided into several discrete number of horseshoe vortices. A horseshoe vortex system consists of three parts of which the bound vortex portion is lied on the lifting line and the other two are trailing vortices. To calculate the induced velocity at any point Biot-Savart law is used. For the calculation of circulation strength ,the induced velocities are calculated at the body control points which are located at the three-quarter chord mean line. The lift, and drag coefficients are

calculated for the hydrofoil by considering the effect of body and image. Also the moment coefficient about the mid point of the mean camber line is calculated. For simplification of calculation, the initial free surface disturbance is assumed zero. The method of solution is based on the criterion of image stabilization hence free surface which is established using a iterative procedure. The lift, drage and moment coefficient for the hydrodoil are calculated at the final iteration. Also the free surface shape is calculated at this final stage. The existing prediction method is not an iterative one i.e., in that method the effect of free surface deflection is not considered when the foil characteristics is calculated. But the method developed is an iterative one to stabilize the free surface i.e., the effect of free surface is considered when the foil characteristics is calculated.

For the purpose of demonstration of different hydrofoil characteristics using method developed NACA 4412 and NACA 16-206 section profile data are used. NACA 4412 section profile is basically chosen for demonstration of performance at high aspect ratio i.e.,equal to or above 5. Whereas NACA 16-206 section profile is basically chosen for demonstrtion of performance at low aspect ratio i.e.,equal to or above 4/3. NACA 4412 is a high lift profile compared with NACA 16-206 which is a low lift profile. For NACA 4412 section profile the comparison is made with available theoretical results.

CONTENTS

NOTATIONS

B	:	Breadth
b	:	Body
Cm,n	:	Influence coefficient
c	:	chord
C_L	:	Lift coefficient
$C_{L\infty}$	:	Lift coefficient without free surface (i.e.,image)
C_D	:	Drag coefficient
C_M	:	Moment coefficient
dC_L	:	Lift coefficient of a strip
dC_D	:	Drag coefficient of a strip
dC_M	:	Moment coefficient of a strip
dSn	:	Width of a strip along span
D	:	Drag force
Fr	:	Froude number based on depth of submergence($V/\sqrt{gh}$)
	:	Froude number based on chord($V/\sqrt{gc}$)
f	:	Free surface
g	:	Acceleration due to gravity
h	:	Depth of submergence
i	:	Image
$\hat{i}$	:	Unit vector in X-direction
$\hat{j}$	:	Unit vector in Y-direction
KO	:	Wave factor (g/V)
$\hat{k}$	:	Unit vector in Z direction
l	:	Lift per unit span

L	:	Total Lift force/Length
M	:	Moment of force
m	:	Number of control points
n	:	Number of strips
P	:	Pressure
r	:	Radius vector
S	:	Span
U_∞	:	Free steam velocity
V	:	Total velocity
Vx	:	Velocity in X-direction
Vy	:	Velocity in Y-direction
Vz	:	Velocity in Z-direction
X1n,X2n	:	X-ordinates of bound vortex point
Xm	:	X-ordinate of control point
Y1n,Y2n	:	Y-ordinates of bound vortex point
Ym	:	Y-ordinate of control point
Z1n,Z2n	:	Z-ordinates of bound vortex point
Zm	:	Z-ordinate of control point
α	:	Angle of attack
Γn	:	Circulation of a strip varies along span
ρ	:	Density of water
ζ	:	Deflection of free water surface
φ	:	Dihedral angle
δ	:	Angle of mean camber line at the control point.
Δ	:	Displacement
θ	:	Angle between two vectors

LIST OF FIGURES

LIST OF TABLES

CHAPTER - 1

INTRODUCTION

1.0 SUMMARY OF THE CHAPTER

The basic definition of hydrofoil and hydrofoil boat are given in this chapter. A comparison between hydrofoil boat and displacement vessel is given to show the power variation at relatively higher speed. The objectives of the present study is to predict hydrofoil characteristics at shallow submergences with some basic assumptions.Literature review describes the work done on this topic.The solution procedure is based on lifting line theory and vortex lattice method. Scope of application shows the various possible usage of hydrofoil boat in this riverine country.

1.1 GENERAL :

Hydrofoil boats make use of the same principle involved in the flight of aircraft. Hydrofoils are attached to the bottom of the ship by means of struts, and when the ship moves through the water a lift force is generated just as occurs when an aeroplane wing moves through the air. By correct adjustment of the angle of incidence of the hydrofoil the lift can be made to be just equal to the weight of the ship, which is lifted clear of the water. The resistance is there by reduced, being then only equal to the drag of the hydrofoils. So high speed can be achieved with relatively low power.

In Table 1.1 [1] [2], a comparison of power absorbed by hydrofoil boat and displacement type ship is provided.Figure 1.2 shows the comparative performance of high-speed craft. Hydrofoil boat has been used for service in sheltered waters but it is likely that considerable problems would exist in really rough water. The definition sketch of a hydrofoil boat is given in Figure 1.1 [3].

Lifting line theory and vortex lattice method are used to solve the problem assuming the hydrofoil with arbitrary profile and plan form, flow is incompressible, inviscid and irrotational with negligible pressure above the free surface, no surface tension, depth of fluid is infinite. Also the solution procedure is based on a iterative process satisfying simultaneously both the boundary condition that the flow is tangential at the body control point and image stabilizing criterion.

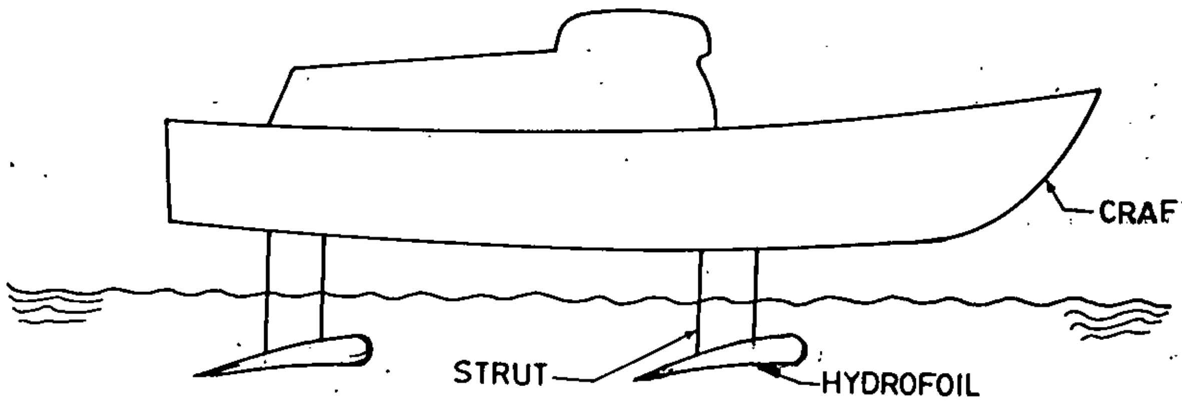

FIG. 1.1 DEFINITION SKETCH OF A HYDROFOIL CRAFT.

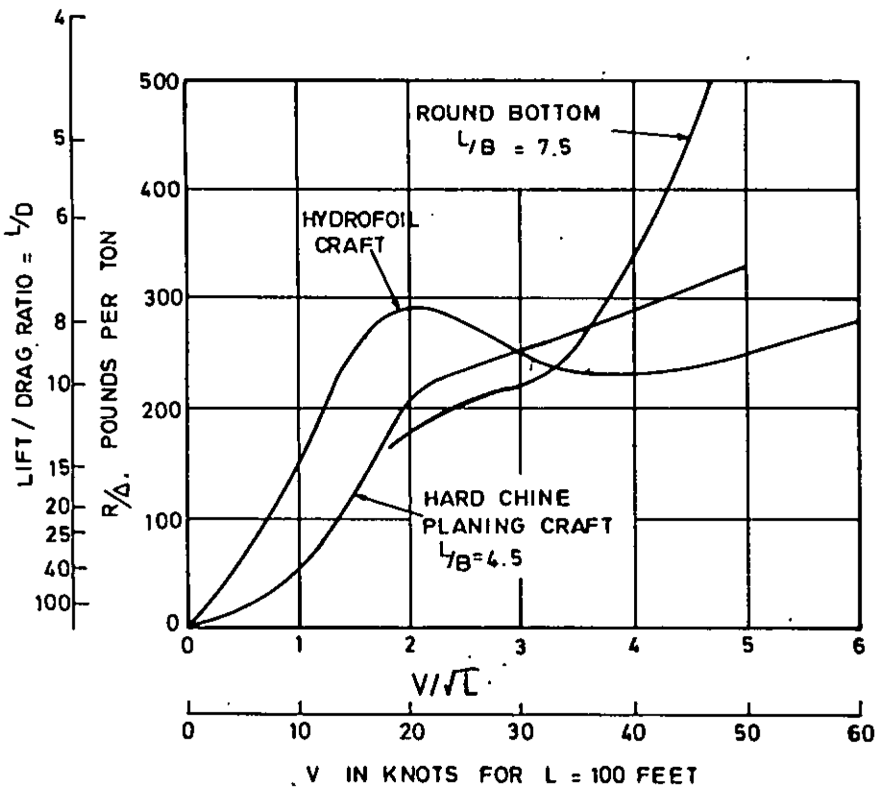

Fig. 1.2. Comparative performance of high-speed craft .

Table - 1.1 : Comparison of power absorbed by hydrofoil boat and displacement type ship

Type of ship	Dimension (meter)	Displacement (tonne)	Velocity (knot)	Power (H.P)
Hydrofoil vessel	Length=40.5 Breadth=8.6 Draught=2.7	247	50	17024
Dispalcement Vessel				18686
Hydrofoil Vessel	Length=30 Breadth=9.4 Draught=1.03	65	36	1581
Displacement Vessel				3218

1.2 OBJECTIVES OF THE PRESENT STUDY :

The objectives of the present study is to develop a proper hydrofoil characteristics prediction method which will take into consideration the variation of speed of flow, angle of attack, depth of submersence and free surface effect. The calculated characteristics are to be compared with the available theoretical results to validate the method developed for prediction .

1.3 LITERATURE REVIEW

The hydrofoil concept has been around for many decades, but much of the early development involved experimental craft and the achievement of viable craft. Eventually viable craft were built to satisfy both commercial ferry and military requirements. This development and involvement continued to the present day, and future prospects look promising. In general, the European and Russian craft employ surface piercing foils, where as well as providing lift, the foils contribute to craft stability at differential immersion. This provides restoring moments, either in pitch or roll. The major American developments use fully submerged foils, which require an automatic control system to maintain the craft hull at a given height above the water surface. In general, the surface piercing hydrofoils are older, more established designs, whereas the fully submerged foil designs are more recent. The former are used extensively, mainly as passenger transports, and the latter have been used both as military and commercial craft. Fully submerged foil craft are generally more complex and costs are higher, and thus whilst performance is extremely good, these higher costs have lead to difficulties in their general adoption.

H. Lamb [5] indicates in 1913 result that the resistance of a circular cylinder (represented by a doublet) moving under a free surface reaches a peak value for a Froude number (based on submergence depth) of unity. This problem has been further studied by T.H. Have lock (1936) [6]; but, from a hydrofoil stand point, consideration of a vortex is of more importance. L.N. Sretensky (1938) [5] extended the analysis to include the effect of circulation and dropped the terms specifying the circular cylinder. When the submersion was greater than three times the cylinder radius, he found that the cylinder could be effectively replaced by a vortex. This work and that by others - N.E. Kotchin for arbitrary contours, and M.V. keldysh and M.A. Lavrentiev (1935) [7] for a wing in Russia in the mid 1930's has been summarized by A.N.Vladimirov (1937), together with indications of experimental verification.

The keldysh and Lavrentiev (1935) and Srentensky (1938) [5] approach replaces the flow indicated in Figure 1.3a by the system indicated in Fig. 1.3b - of a negatively sensed vortex at the foil location, its "biplane" image located at a distance h above the nominal free - surface location, together with additional terms involving Froude number effects. These latter terms are appropriately called the "gravity image" by A.G. Strandhagen and G.R. Seikel (1957). Joseph P. Geising and A.M.O. Smith (1967) [8] adopt this image formation procedure to solve the potential flow about two dimensional hydrofoils.

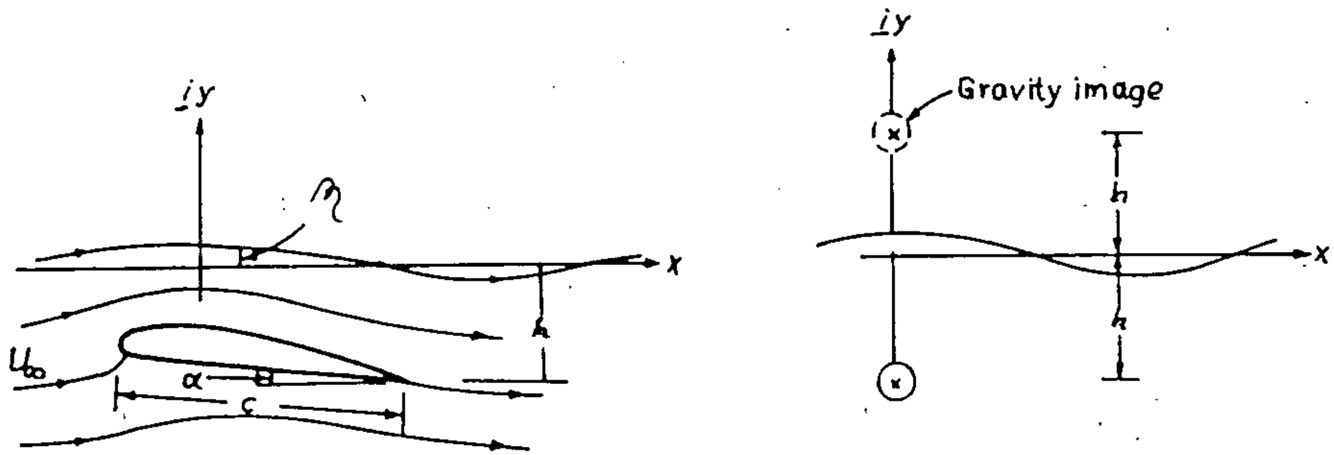

(a) Flow pattern

(b) Singularity and image system.

FIG. 1.3 : FLOW DEPICTION ABOUT FOIL NEAR FREE SURFACE.

1.4. ADOPTED SOLUTION PROCEDURE

The study is based on lifting line theory and vortex lattice method. Lifting line theory representation is that the hydrofoil is replaced by a bound vortex line located at the quarter chord location (hydrodynamic center of the foil). In vortex lattice method the hydrofoil is divided into several trapezoidal panels (also called finite elements or lattices) along the span. The individual three sided horseshoe vortices which consist of bound vortex and trailing vortex are placed in that trapezoidal panels. The bound vortex coincides with the quarter chord line of the panel (or element). To calculate the foil characteristics, control points are located at the three-quarter chord. In rigorous theoretical analysis, the vortex lattice panels are located on the mean camber surface of the wing and, when the trailing vortices leave the wing, they follow a curved path. But in many engineering applications, suitable accuracy can be obtained using linearized theory in which straight line trailing vortices extend downstream to infinity. To evaluate the induced velocity components circulation strength is required. To compute the circulation strengths of the vortices , which represent the lifting flow field of the wing, it is used the boundary condition that the surface is a streamline. That is, the resultant flow is tangential to the wing at each and every control point (which is located at the midspan of the three-quarter chord line of each elemental panel).

In this solution procedure it is assumed that there will be an image of the hydrofoil at a distance of submergence (h) from the interface when the hydrofoil is submerged to depth h. To calculate the induced velocity and circulation strength this image effect would be considered. It is assumed that there is a bound vortex line at the image on the three-quarter chord line. The addition of this bound vortex line effect with the body bound vortex line gives the actual characteristics of the hydrofoil.

To simplify the calculation firstly it is assumed that the free water surface is undisturbed which acts as a reflector. Due to the hydrofoil motion the free water surface deflection is calculated by applying Bernoulli's equation. As the free water surface is disturbed, the formed image of the hydrofoil will be distorted. This study is based on image stabilizing criterion. To stabilize the image, it is assumed that if the free water surface is stable, the formed image will be stable.

In the image stabilizing criterion, the free - water surface deflection at the quarter chord line is considered. If this deflection rate is very small (less than 0.1 percent) it is assumed that the free water surface is stable which is the image stabilizing criterion. A schematic diagram of the solution procedure is given below.

Prediction of finite span hydrofoil characteristics using image stabilizing criterion.

↓

The calculation procedure involves lifting line theory, vortex lattice method, Biot-Savart law and image stabilizing criterion.

↓

The major assumptions are : (a) Considering the hydrofoil with arbitrary profile and plan form. (b) The flow is assumed to be incompressible, inviscid and irrotational with negligible pressure above the free surface. (c) Surface tension is ignored. (d) The depth of fluid is infinite. (e) To stabilize the image the percentage of free water surface deflection at the quarter chord line is less than 0.1 .

↓

Results are :

Calculation of		Speed of flow
lift force,	Against variation of	Angle of attack
drag force &		Depth of submergence
Moment of force		

↓

Comparison with the available theoretical results to validate the developed prediction method.

1.5 SCOPE OF APPLICATION :

Our country is a riverine one and also got a long coastline.To reach a distant place in a shorter possible time a more stable and speedy vessel is required. But from economic point of view to design a speedy displacement type vessel is costly. Because more than 90 percent of total hull resistance of a submersible vessel is frictional resistance and wave making resistance. To reduce these resistances, the concept of hydrofoil boat (a boat with a hydrofoil) emerge. The body of the hydrofoil boat is above the water surface and only the hydrofoil is under the water surface. So, the resistance is thereby reduced, being then equal to the drag of the hydrofoil. The result is that high speed is possible without using unduly large power. hydrofoil boat may be used in the following fields.

(a) Coast guard craft

(b) Rescue craft

(c) Speedy passenger craft for better river communication .

CHAPTER -2

THEORY AND METHOD OF SOLUTION

2.0 SUMMARY OF THE CHAPTER

The developed theory to predict the foil characteristics is presented in this chapter.To solve the circulation matrix equations the boundary condition used is that the flow is tangential at three-quarter chord line.Method of solution based on numerical computations using the theory developed for a specific hydrofoil is described with a flow chart.

2.1 THE THEORY

To attempt a general solution of the problem of determining a vortex system by representing a finite wing is very difficult. However, the simplified system of a horseshoe vortex is accurate enough only for certain special problems. It can be improved on the accuracy of the system by using a different representation first suggested by Lanchester, and subsequently fully analysed by Prandtl [9], in which the bound vorticity is assumed to lie on a straight line joining the quarter chord line of the wing, known as the lifting line .

Lifting line theory provides a reasonable estimate of the lift, drag and the induced velocity for an unswept wing of relatively moderate or high aspect ratio in a subsonic stream. It is assumed that the resultant flow is to be steady, inviscid, irrotational, and incompressible. In this approach to solve the governing equation, the continuous distribution of bound vorticity over the wing surface is approximated by a finite number of discrete horseshoe vortices of which each consists of three straight segments. The individual horseshoe vortices are placed in trapezoidal panels (also called finite elements or lattices). Hence, this procedure for obtaining a numerical solution to the flow is termed the vortex lattice method (VLM).

The hydrodynamic centre is that point about which the section moment coefficient is independent of the angle of attack. The quarter chord location is significant since it is the theoretical hydrodynamic centre for incompressible flow about a three-dimensional hydrofoil. The bound vortex coincides with the quarter chord line of the panel (or element). In a rigorous theoretical analysis, the vortex lattice panels are located on the mean camber surface of the wing and, when the trailing vortices leave the wing, they follow a curved path. However, for many engineering applications, suitable accuracy can be obtained using linearized theory in which straight line trailing vortices extend downstream to infinity. In the linearized approach the trailing vortices are aligned either parallel to the free stream or parallel to the vehicle axis.

Both orientations provide similar accuracy within the assumptions of linearized theory. In this study, it is assumed that the trailing vortices are parallel to the axis of the vehicle. Application of the boundary condition is that the flow is tangent to the wing surface at the control point of each of the N panels provides a set of simultaneous equations in the unknown vortex circulation strengths. The control point of each panel is centered spanwise on the three-quarter chord line midway between the trailing vortex legs.

An indication of why the three-quarter chord location is used as the control point may be seen by referring to Fig.2.1. A vortex filament whose circulation strength represents the lifting character of the section is placed at the quarter chord location. Using linearized theory it induces a velocity $V = \Gamma / 2\pi r$, at a point C, the control point which is a distance r from the vortex filament. If the flow is to be parallel to the surface at the control point, the incidence of the surface relative to the free stream is given by

$$\alpha = \sin\alpha = V/U_\infty = \Gamma/2\pi r U_\infty \qquad \text{..........} (2.1)$$

Now using the equaiton of lift per unit span.

$$l = \frac{1}{2}\rho U_\infty^2 c C_L = \rho U_\infty \Gamma \qquad \text{.............}(2.2)$$

using for thin foil $C_L = 2\pi\alpha$

$$l = \frac{1}{2}\rho U_\infty^2 c\, 2\pi\alpha$$

Combining the relations above.

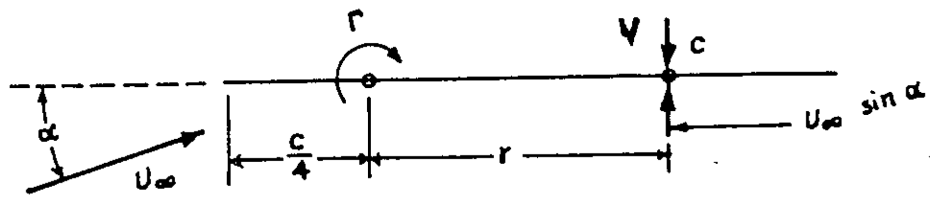

FIG. 2.1: SKETCH OF A PLANER HYDROFOIL SECTION INDICATING LOCATION OF CONTROL POINT WHERE FLOW IS PARALLEL TO THE SURFACE.

$$\pi \rho U_\infty^2 c \frac{\Gamma}{2\pi r U_\infty} = \rho U_\infty \Gamma$$

solving for r, $r = c/2$

Thus it is found that the control point is at the three-quarter chord location by assuming that the bound vortex and control point are on a straight line.

To compute the circulation of a specific finite element the image effect would be considered. And this study is based on image stabilizing criterion. It is assumed that, there will be an image at a height of equal depth of the hydrfoil above the interface shown in Figure 2.2. Bound vortex line is assumed at the quarter chord line of the image. For a specific finite element the total (actual) lift is the summation of body bound vortices and image bound vortices effect. To simplify the calculation, first it is assumed that the free water surface is undisturbed. Applying Bernoulli's equation the height of the disturbed free water surface is calculated.

This solution procedure is based on the image stabilizing criterion. The image is stabilized by converging the free water surface deflection at quarter chord locaion. At the first time (first iteration) of deflection calculation procedure, it is assumed that the free water surface is undisturbed which acts as a reflector. As it is assumed that there will be an image at a distance h from the

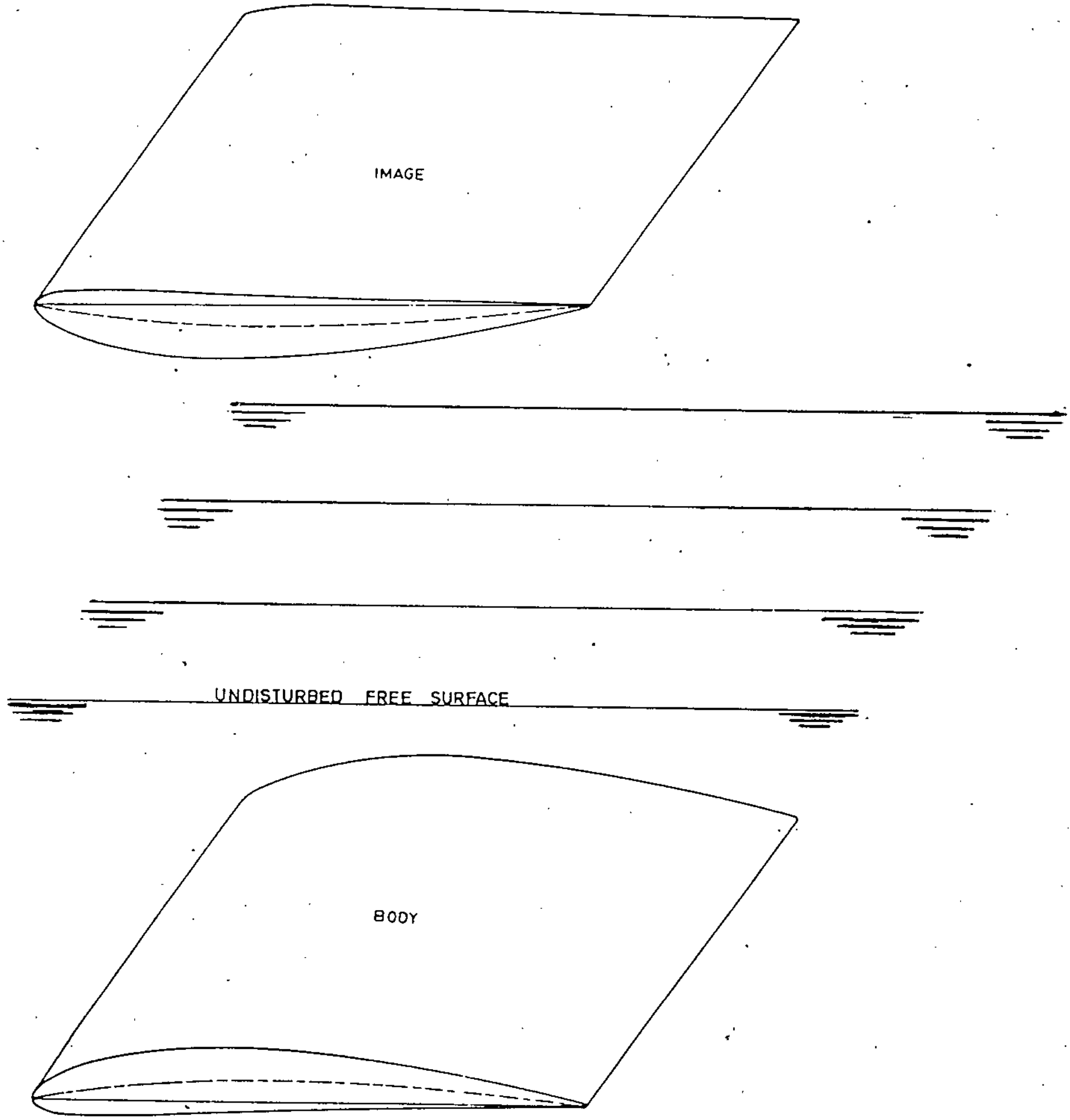

FIG. 2.2 : HYDROFOIL AND IMAGE WITH UNDISTURBED FREE SURFACE.

interface when the hydrofoil is submerged at a depth h in water, the image is undistorted for this free water surface position. When the free water surface is deflected, the formed image also distorted. To stabilize the image different iterations are required. In this study it is assumed that, when the free water surface deflection at the quarter chord location is less than 0.1 percent in compared to the preceeding iteration the formed image is stable, so the accuracy of this process depends on the quarter chord location free water surface deflection.

2.2 BOUNDARY CONDITION

To compute the strengths of the vortices which represents the lifting flow field of the wing the boundary condition used is that the surface is a streamline. That is, the resultant flow is tangent to the wing at each and every control point which is located at the midspan of the three-quarter chord line of each elemental panel. If the flow is tangent to the wing, the component of the induced velocity normal to the wing at the control point balances the normal component of the free stream velocity. To evaluate the induced velocity components, the convention introduced is that the trailing vortices are parallel to the chord line (i.e. velocity in X-direction)

Referring to Fig. (2.3)......, the tangency requirement yields the relation

$$-V_X \sin\delta \cos\varphi - V_Y \cos\delta \sin\varphi + V_Z \cos\varphi \cos\delta + U_\infty \sin(\alpha-\delta)\cos\varphi = 0 \quad \ldots(2.3)$$

where, α = Angle of attack

φ = Dihedral angle

δ = Slope of the control point at mean camber line.

After rearrangement, it may be written in the form,

$$\frac{1}{\sin(\alpha-\delta)}\left[V_X \sin\delta + V_Y \cos\delta \tan\varphi - V_Z \cos\delta\right] = U_\infty \quad \ldots\ldots(2.4)$$

Now for a specific wing moving at any angle with velocity U_∞, equation (2.4) gives N (number of strip) numebr linear equations.

In this study these linear equations are solved by Gauss Seidel [11] Matrix equation method.

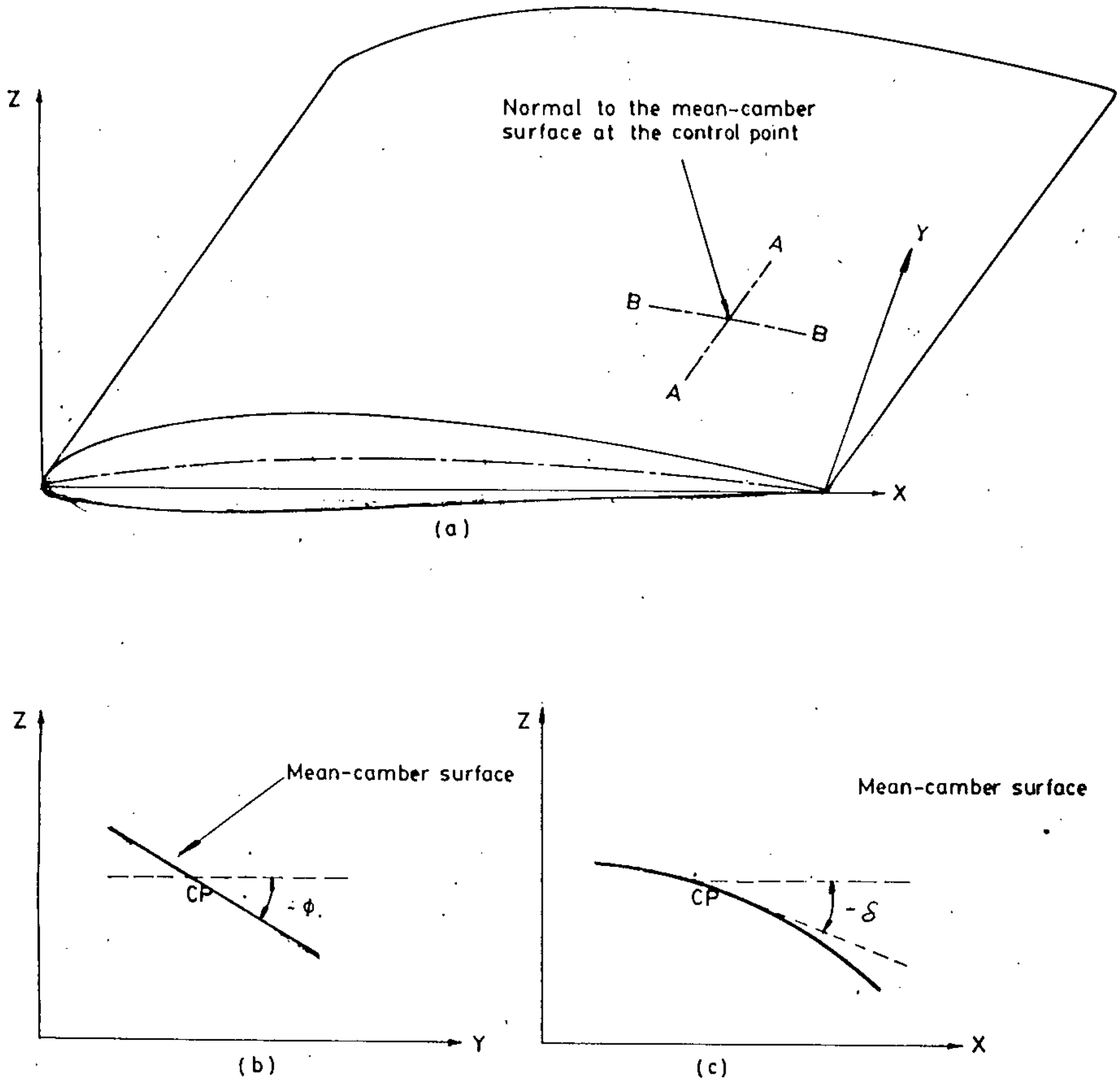

FIG. 2.3 : NOMENCLATURE FOR THE TANGENCY REQUIREMENT : (a) NORMAL TO ELEMENT OF THE MEAN-CAMBER SURFACE : (b) SECTION AA : (c) SECTION BB .

2.3 METHOD OF SOLUTION

The method of solution is based on lifting line theory and vortex lattice method. The induced velocity expressions are based on Biot-Savart law and involves circulation strengths of vortex elements and location of vortex elements and control points .Initially the circulation strengths are unknown and later found by solving particular equation using Gauss-Seidel [11] method.By knowing the circulation of a particular strip, the induced velocity can be calculated. For the free surface deflection calculation, the induced velocity at the free surface should be known by considering the body and image applying Bernoulli's equaiton on the free surface. To simplify the solution, first it is assumed that the free water surface is undisturbed. When the hydrofoil moves the free water surface is disturbed. By finding this deflection rate in percentage the image stabilizing criterion is fixed which is equal to 0.1 percent. The overall method of solution is described below by a flow chart.

Given chord, span, coordinates of bound vortex and control points, velocity, angles (flow, dihedral and at the control point of mean camber line) and no. of iterations.

↓

Assume initially disturbed free surface with zero deflection.

↓

Formation of circulation matrix using Biot-Savart law.

↓

Calculation of induced velocity at the body control points by solving the circulation matrix using Gauss-Seidel method.

↓

Calculation of lift, drag and moment coefficients.

↓

calculation of induced velocity and deflection( ) at the free surface.

↓

Convergence test of deflection rate with 0.001

↓

If the deflection rate does not satisfy the above criterion repeat the calculation by changing the recent Z-coordinate of image.

CHAPTER - 3

INDUCED VELOCITY DERIVATION

3.0 SUMMARY OF THE CHAPTER

This chapter consists of detailed development procedure of the theory .A horseshoe vortex lattice consists of three parts , one is bound vortex and the other two are trailing vortices.The induced velocity by the bound vortex and the trailing vortex at the control point is calculated by using Biot-Savart law.The total induced velocity at any control point is the summation of velocity induced by the body and image.

3.1. CALCULATION OF THE INDUCED VELOCITY BY A FINITE LENGTH VORTEX SEGMENT.

To determine the flow about a vortex loop of arbitrary form, it is necessary to have a way of finding the velocities given to the fluid at various points by each of the elementary segments of which the loop is made up. Biot-Savart law relates the intensity of flow in the fluid close to a 'vorticity carrying' vortex tube to the strength of the vortex tube. In this approach the continuous distribution of bound vorticity over the wing surface is approximated by a finite number of discrete horseshoe vortices of which each consists of three straight segments to solve the governing equation.

The individual horseshoe vortices are placed in trapezoidal panels. A horseshoe vortices system consists of three segments. One segment is bounded by two end points of the trapezoidal panel named bound vortex and the other two are trailing vortices. The velocity induced by a vortex filament of strength Γn and a length $\vec{dl}$ is given by the law of Biot-Savart [10] as

$$d\vec{v} = \Gamma n \, (\vec{dl} \times \vec{r}) / 4 \pi \vec{r} \ldots\ldots\ldots\ldots (3.1)$$

From figure (3.1) the magnitude of the induced velocity is

$$dv = \Gamma n \, \mathrm{Sin}\theta \; dl \, / \, 4 \pi \, r^2 \ldots\ldots\ldots\ldots\ldots (3.2)$$

Now to calculate the effect of each segment separately, let AB be such a segment, with the velocity vector directed from A to B and let C be a point in space, whose normal distance from the line AB is rp.

$$r = rp/\sin\theta \;,\; dl = rp \,\mathrm{cosec}^2 \theta \; d\theta.$$

Integrating between A and B to find the magnitude of the induced velocity,

$$V = \Gamma n/4\pi r_p \int_{\theta 1}^{\theta 2} \mathrm{Sin}\theta \, d\theta = \Gamma n/4\pi r_p \; (\cos\theta_1 - \cos\theta_2) \ldots (3.3)$$

Now, if the vortex filament extends to infinity in both directions, then $\theta 1 = 0$ and $\theta 2 = \pi$.

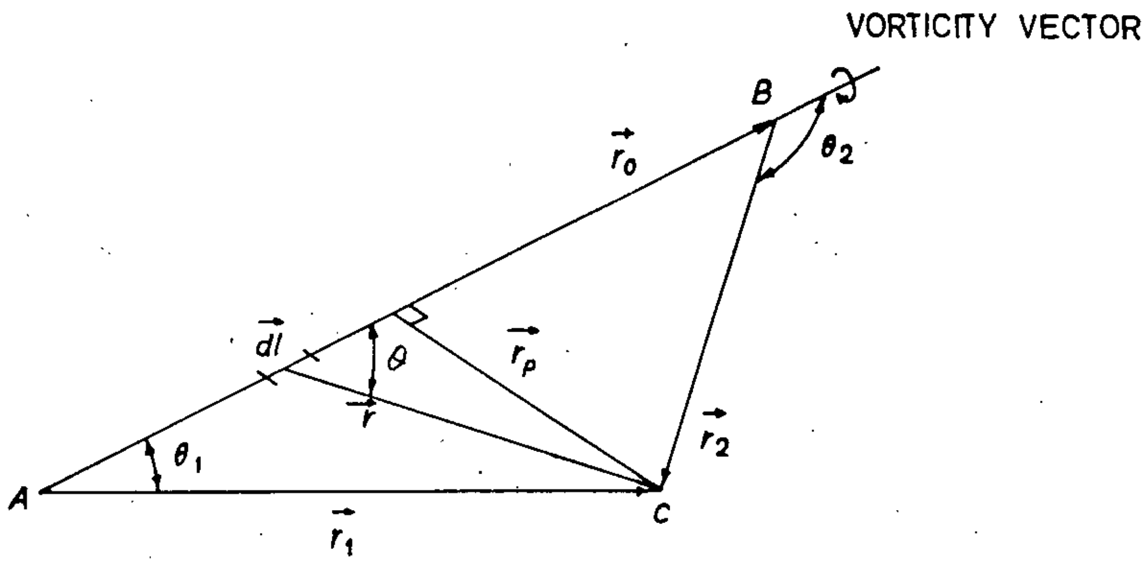

FIG. 3.1 : NOMENCLATURE FOR CALCULATING THE VELOCITY INDUCED BY A FINITE LENGTH VORTEX SEGMENT.

Now, in this case, $V = \Gamma n / 2 r_p \pi$

Let $\vec{ro}$, $\vec{r1}$ and $\vec{r2}$ represent the vectors AB, AC and BC **respectively.**

Then $rp = |\vec{r1} \times \vec{r2}| / ro$.

$\cos \theta 1 = \vec{ro} . \vec{r1} / ro\ r1$, $\cos \theta 2 = \vec{ro} . \vec{r2} / ro\ r2$

and consider unit vector is $\vec{r1} \times \vec{r2} / |\vec{r1} \times \vec{r2}|$

Substituting these expressions into equation (3.3) **and noting that** the direction of the induced velocity is **given by the unit vector** $(\vec{r1} \times \vec{r2}) / |\vec{r1} \times \vec{r2}|$ yields,

$$\vec{V} = \{\Gamma n / 4\pi\} \{(\vec{r1} \times \vec{r2}) / |\vec{r1} \times \vec{r2}|\} \{\vec{ro} . (\vec{r1}/r1 - \vec{r2}/r2)\} \ldots\ldots (3.4)$$

This is the basic expression for the calculation **of the induced** velocity by the horse shoe vortices in the vortex lattice **method.**

3.2. VELOCITY INDUCED BY BOUND VORTEX PORTION OF HORSESHOE SYSTEM

Equation (3.4) is used to calculate the velocity that is induced at a general point in space (X,Y,Z) by the horseshoe vortex shown in Figure 3.2.This horseshoe vortex may be assumed to represent that for a typical wing panel.Segment AB represents the bound vortex portion of the horseshoe system and coincides with the quarter chord line of the panel element. For the bound vortex segment AB,

$$\vec{ro} = \vec{AB} = (X2n - X1n)\,\hat{i} + (Y2n - Y1n)\,\hat{j} + (Z2n\ Z1n)\,\hat{k}$$

$$\vec{r1} = (X-X1n)\,\hat{i} + (Y-Y1n)\,\hat{j} + (Z-Z1n)\,\hat{k}$$

$$\vec{r2} = (X-X2n)\,\hat{i} + (Y-Y2n)\,\hat{j} + (Z-Z2n)\,\hat{k}$$

using equation (3.4) to calculate the velocity induced at some point C(X,Y,Z) by the vortex filament AB (shown in Figs. 3.2 and 3.3), it is seen that

$$\vec{VAB} = \Gamma n/4\pi\ \{Fac1AB\}\ (Fac2AB\} \ldots\ldots\ (3.5)$$

where, $\{Fac\ 1AB\} = |\vec{r1} \times \vec{r2}| / |\vec{r1} \times \vec{r2}|$

and $\{Fac\ 2AB\} = \{(\vec{ro}.\ \vec{r1} / r1) - (\vec{ro}.\ \vec{r2}/r2)\}$

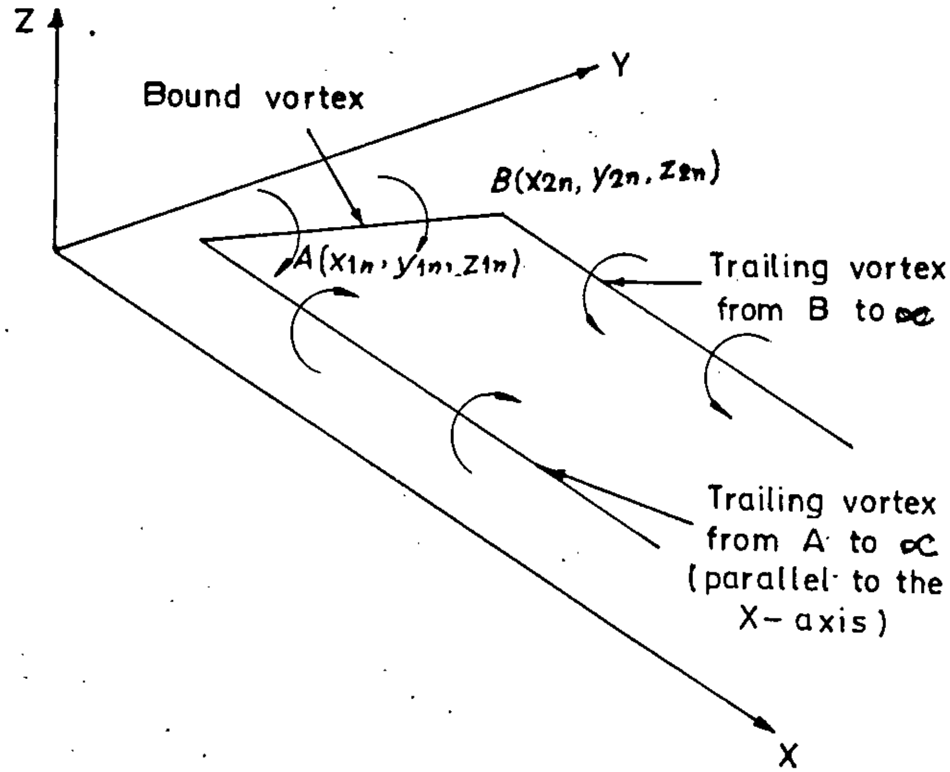

FIG. 3.2: SKETCH OF A "TYPICAL" HORSESHOE VORTEX.

The cross product of $\vec{r1}$ and $\vec{r2}$ vector is

$$\vec{r1} \times \vec{r2} = [\{(Y-Y1n)(Z-Z2n) - (Y-Y2n)(Z-Z1n)\}\hat{i} - \{(X-X1n)(Z-Z2n) - (X-X2n)(Z-Z-1n)\}\hat{j} + \{(X-X1n)(Y-Y2n) - (X-X2n)(Y-Y1n)\}\hat{k}]$$

The magnitude of this cross product is

$$|r1 \times r2|^2 = [\{(Y-Y1n)(Z-Z2n)-(Y-Y2n)(Z-Z1n)\}^2 + \{(X-X1n)(Z-Z2n)-(X-X2n)(Z-Z1n)\}^2 + \{(X-X1n)(Y-Y2n)-(X-X2n)(Y-Y1n)\}^2].$$

Thus. { Fac1AB} becomes,

$$\{Fac1AB\} = \{[(Y-Y1n)(Z-Z2n)-(Y-Y2n)(Z-Z1n)]\hat{i} - [(X-X1n)(Z-Z2n) - (X-X2n)(Z-Z1n)]\hat{j} + [(X-X1n)(Y-Y2n) - (X-X2n)(Y-Y1n)]\hat{k}\}/\{[(Y-Y1n)(Z-Z2n) - (Y-Y2n)(Z-Z1n)]^2 + (X-X1n)(Z-Z2n) - (X-X2n)(Z-Z1n)]^2 + [(X-X1n)(Y-Y2n) - (X-X2n)(Y-Y1n)]^2\}$$

Using the principle of dot product of vector { Fac 2AB} becomes,

$$\{Fac\ 2AB\} = \{[(X2n - X1n)(X-X1n) + (Y2n-Y1n)(Y-Y1n) + (Z2n-Z1n)(Z-Z1n)]/\sqrt{[(X-X1n) + (Y-Y1n) + (Z - Z1n)]^2} - [(X2n-X1n)(X-X2n) + (Y2n-Y1n)(Y-Y2n) + (Z2n - Z1n)(Z-Z2n)]/\sqrt{[(X-X2n) + (Y-Y2n) + Z-Z2n)]^2}\}$$

Using the above relationships equation (3.5) can be written as,

$$VAB = (\Gamma n/4\pi)\ \{Fac1AB\}\{Fac\ 2AB\}.....(3.5)$$

$$= (\Gamma n/4\pi)\ \{[(Y-Y1n)(Z-Z2n)-(Y-Y2n)(Z-Z1n)]\hat{i} - [(X-X1n)(Z-Z2n)-(X-X2n)(Z-Z1n)]\hat{j} + [(X-X1n)(Y-Y2n)-(X-X2n)(Y-Y1n)]\hat{k}\}/\{[(Y-Y1n)(Z-Z2n)-(Y-Y2n)(Z-Z1n)]^2 + [(X-X1n)(Z-Z2n)-(X-X2n)(Z-Z1n)]^2 + [(X-X1n)(Y-Y2n)-(X-X2n)(Y-Y1n)]^2\}\ \{[(X2n-X1n)(X-X1n)+(Y2n-Y1n)(Y-Y1n)+(Z2n-Z1n)(Z-Z1n)]/\sqrt{[(X-X1n)^2+(Y-Y1n)^2+(Z-Z1n)^2]} - [(X2n-X1n)(X-X2n)+(Y2n-Y1n)(Y-Y2n)+(Z2n-Z1n)(Z-Z2n)]/\sqrt{[(X-X2n)^2+(Y-Y2n)^2+(Z-Z2n)^2]}\}..........(3.6)$$

Let,

$$C = [(Y-Y1n)(Z-Z2n)-(Y-Y2n)(Z-Z1n)]$$

$$D = [(X-X1n)(Z-Z2n)-(X-X2n)(Z-Z1n)]$$

$$E = [(X-X1n)(Y-Y2n)-(X-X2n)(Y-Y1n)]$$

$$F = [(X2n-X1n)(X-X1n)+(Y2n-Y1n)(Y-Y1n)+(Z2n-Z1n)(Z-Z1n)]$$

$$G = [(X2n-X1n)(X-X2n)+(Y2n-Y1n)(Y-Y2n)+(Z2n-Z1n)(Z-Z2n)$$

$$H = \sqrt{(X-X1n)^2+(Y-Y1n)^2+(Z-Z1n)^2}$$

$$P = \sqrt{(X-X2n)^2+(Y-Y2n)^2+(Z-Z2n)^2}$$

Thus equation (3.6) becomes with these substitutions

$$\vec{VAB} = (\Gamma n/4\pi)\{[C\hat{i} - D\hat{j} + E\hat{k}]/(C^2 + D^2 + V^2)\}\{F/H - G/P\}.........(3.7)$$

3.3 VELOCITY INDUCED BY TRAILING VORTEX OF HORSESHOE SYSTEM

To calculate the velocity induced by the filament that extends from A to ∞, let us first calculate the velocity induced by the collinear, finite length filament that extends from A to D. Since $\vec{ro}$ is in the direction of the vorticity vector,

$$\vec{ro} = \vec{DA} = (X1n - X3n)\,\hat{i}$$
$$\vec{r1} = (X - X3n)\,\hat{i} + (Y - Y1n)\,\hat{j} + (Z - Z1n)\,\hat{k}$$
$$\vec{r2} = (X - X1n)\,\hat{i} + (Y - Y1n)\,\hat{j} + (Z - Z1n)\,\hat{k}$$

as shown in Fig.(3.4) . Thus the induced velocity is

$$\vec{VAD} = \Gamma n/4\pi \,\{ Fac\ 1AD \}\,\{ Fac\ 2AD \}$$

where,

$$\{Fac1AD\} = (Z-Z1n)\hat{j}+(Y1n-Y)\hat{k}/[(Z-Z1n)^2+(Y1n-Y)^2]x(X3n-X1n)$$

$$\{Fac2AD\} = (X3n-X1n)\{(X3n-X)/\sqrt{(X-X3n)^2+(Y-Y1n)^2+(Z-Z1n)^2}+ (X-X1n)/\sqrt{(X-X1n)^2+(Y-Y1n)^2+(Z-Z1n)^2}$$

Letting X3 go to ∞, the first term of { Fac 2AD} goes to 1.0. Therefore, the velocity induced by the vortex filament which extends from A to ∞ in a positive direction parallel to the X axis is given by

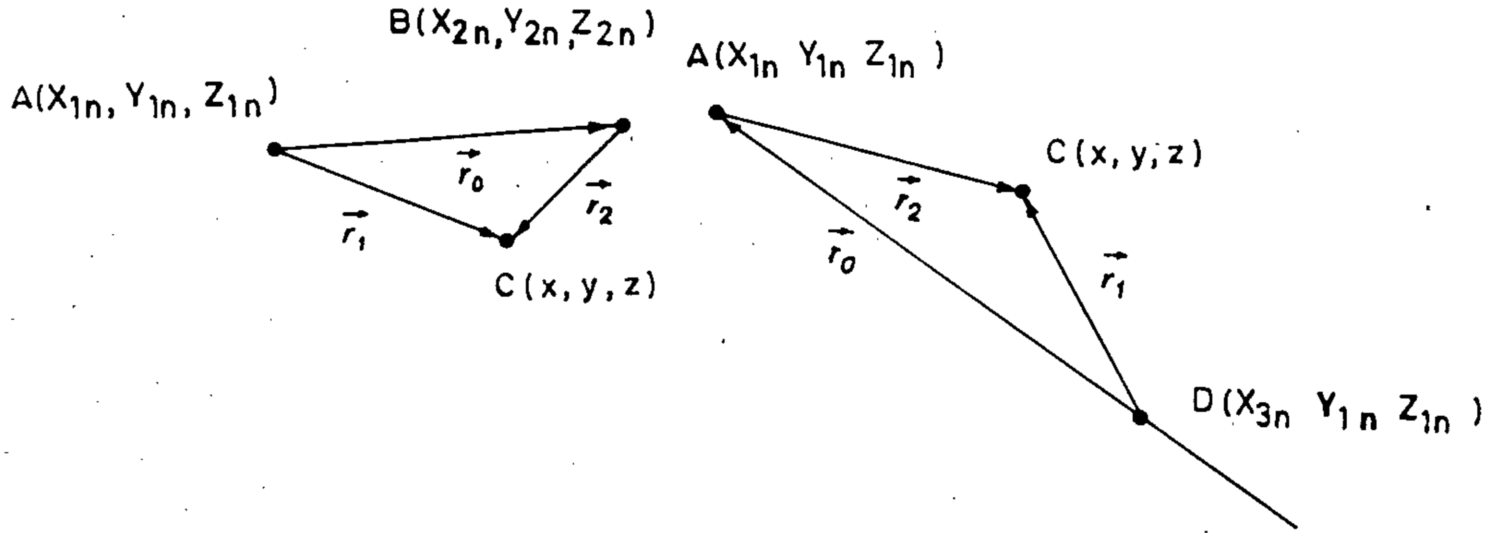

FIG. 3.3 : SKETCH OF THE VECTOR ELEMENTS FOR THE CALCULATION OF THE INDUCED VELOCITIES.

$$VA_\infty = (\Gamma n/4\pi)\{(Z-Z1n)\hat{j} + (Y1n-Y)\hat{k}/((Z-Z1n)^2 + (Y1n - Y)^2)[\ 1.0 + (X-X1n)/\sqrt{(X-X1n)^2 + (Y-Y1n)^2 + (Z-Z1n)^2}\,] \qquad \text{.............(3.8)}$$

Similarly, the velocity induced by the vortex filament that extends from B to ∞ in a positive direction parallel to the X-axis is given by

$$\vec{VB}_\infty = -\Gamma n/4\pi\ \{\ (Z-Z2n)\hat{j} + (Y2n-Y)\hat{k}\ /\ [(Z-Z2n)^2 + (Y2n - Y)^2\,]\ x\ [1.0 + (X-X2n)/\sqrt{(X-X2n)^2 + (Y-Y2n)^2 + (Z-Z2n)^2}\,] \qquad \text{......(3.9).}$$

3.4. EXPRESSIONS FOR TOTAL INDUCED VELOCITY AT THE CONTROL POINTS OF THE HYDROFOIL.

The total velocity induced at a particular control point (Xm,Ym,Zm) by the horseshoe vortex representing one of the surface element and its related image is

$$Vm,n = (\ VAB+\ VA\ \ +VB\ \ )body + (\ VAB+VA\ \ +VB'\ \ )image \qquad \text{...(3.10)}$$

Using equation (3.6),(3.8) & (3.9) the total induced velocity may be calculated using equation(3.10) as follows represented as follows

$$\vec{V}_{m,n} = (\Gamma n/4\pi)\{CS\hat{i}/T + \hat{j}(CC-DS/T)+(ES/T+DD)\hat{k}\}$$
$$= (\Gamma n/4\pi)\ \{\hat{i}U + \hat{j}V + \hat{k}W\}\ldots\ldots\ldots\ldots(3.11)$$

where,

$U = CS/T$

$V = CC-DS/T$

$W = ES/T+DD$

$Q = (Z-Z1n)^2+(Y1n-Y)^2$

$R = (Z-Z2n)^2+(Y2n-Y)^2$

$S = F/H - G/P$

$T = C^2 + D^2 + E^2$

$CC = (Z - Z1n)/P\ \{1+(X-X1n)/G\}-\{(Z-Z2n)/Q\}\ \{1+(X-X2n/H)\}$

$DD = (Y1n-Y)/P\{\ 1 +(X-X1n)/G\}-\{(Y2n-Y)/Q\}\ \{1+(X-X2n)/H\}$

From equation (3.11) it is seen that the X,Y and Z component of induced velocity are the coefficients of $\hat{i}$, $\hat{j}$ and $\hat{k}$ respectively. Assuming these components are,

$VX = \Gamma nCS/4\pi T$

$VY = \Gamma n\ (CC - DS)/\ 4\pi T$

$VZ = \Gamma n\ (ES/T + DD)\ /\ 4\pi$

Yields equation (3.10).

$$\vec{V}_{m,n} = \hat{i}VX + \hat{j}VY + \hat{k}VZ \quad \ldots\ldots\ldots\ldots\ldots\ldots(3.12).$$

The total velocity induced at some point (X,Y,Z) by the horseshoe vortex representing one of the surface elements (i.e., for nth panel) is the sum of the components given in equation (3.6), (3.8) and (3.9). Let the point (X,Y,Z) be the control point of the mth panel, which will be designated by the coordinates (Xm, Ym, Zm). The velocity induced at the mth control point by the vortex representing the nth panel (both body and image) will be designated as Vm,n. Examining equation (3.6), (3.8) and (3.9) it is seen that -

$$\vec{V}_{m,n} = \vec{C}_{m,nb}\,\Gamma_n + \vec{C}_{m,ni}\,\Gamma_n \quad \ldots\ldots\ldots\ldots\ldots(3.13)$$

where the influence coefficient Cm,nb and Cm,ni depends on the geometry of the nth horseshoe vortex and its image distance from the control point of the mth panel. Since the governing equation is linear, the velocities induced by the 2N vortices are added together to obtain an expression for the total induced velocity at the mth control point .

$$\vec{V}_m = (\vec{C}_{m,nb} + \vec{C}_{m,ni})\,\Gamma_n \quad \ldots\ldots(3.14)$$

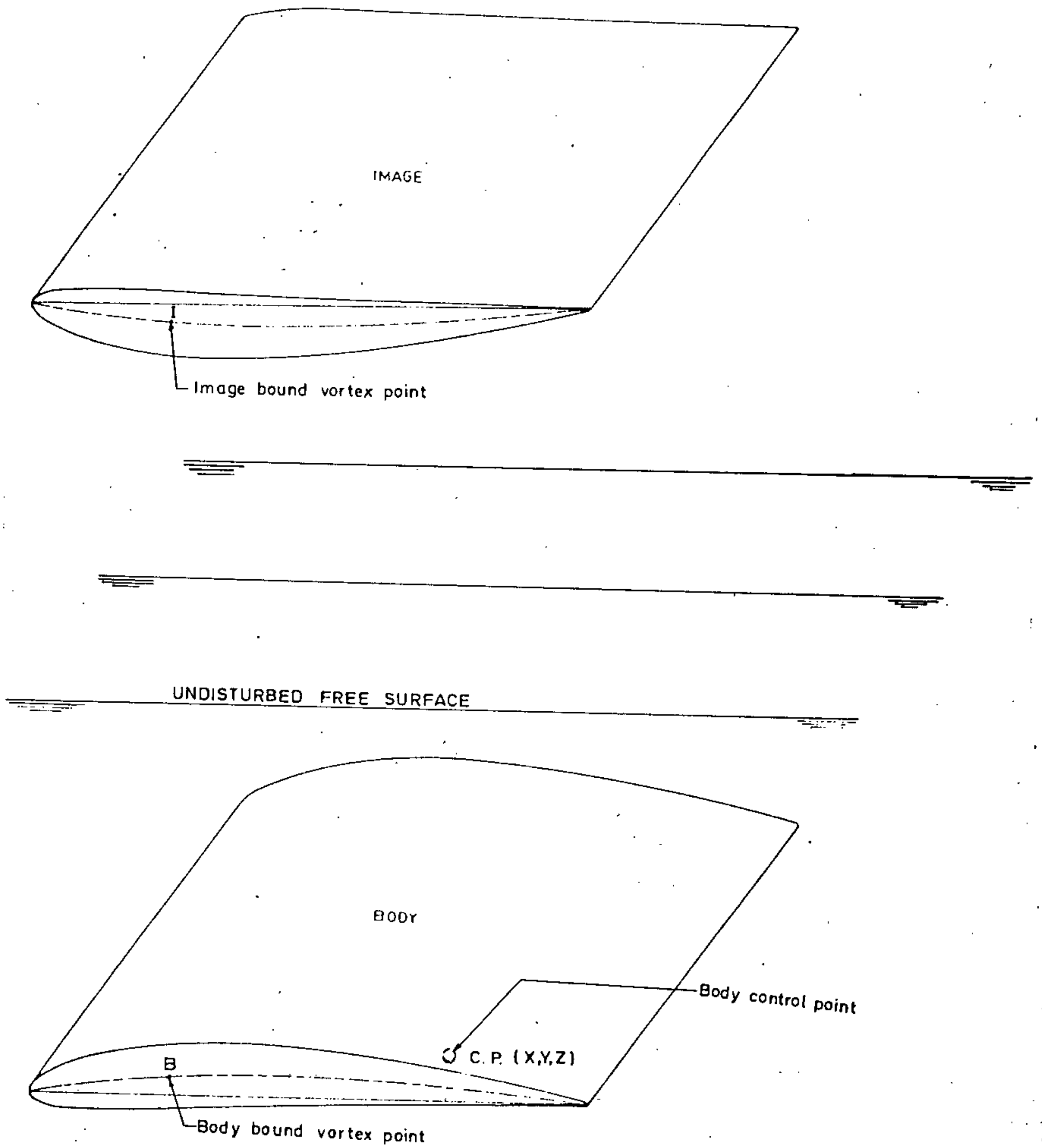

FIG. 3.4 : SHOWING A TYPICAL BODY CONTROL POINT WHERE THE INDUCED VELOCITY IS CALCULATED DUE TO TYPICAL BODY AND IMAGE BOUND VORTEX ELEMENT.

3.5 EXPRESSIONS FOR TOTAL INDUCED VELOCITY AT THE FREE SURFACE :

As this approach is based on image stabilizing criterion, it is assumed that when the hydrofoil is at a depth h, there will be an image at a distance 2h from the hydrofoil in the air which is shown in figure 3.4. Figure 3.5 shows a hydrofoil with body and free surface control point. Like on the hydrofoil it is assumed that there will be a bound vortex line on the image at the quarter chord mean line. But the control points line are remained on the body as before. To compute the total induced velocity at a point on the free surface say A, the effect of body bound vortices (point B) and image bound vortices (point I) would be summed. It is clear that the coordinates of image bound vortices vary from the body only by the Z-coordinates. To ease the calculation, first it is assumed that the free surface is undisturbed. So the Z-coordinate of the image bound vortices is 2(h-Zln).

Let the point (X,Y,Z) be a point at the free surface which will be designated by the coordinates (Xf, Yf, Zf). The velocity induced at the fth point of the free surface by the vortex representing the nth panel will be designated as Vf,n. Examining equation (3.13), it can be seen that,

$$\vec{V}_{f,n} = \vec{C}_{f,nb}\,\Gamma_n + \vec{C}_{f,ni}\,\Gamma_n \qquad \text{.....................(3.15)}$$

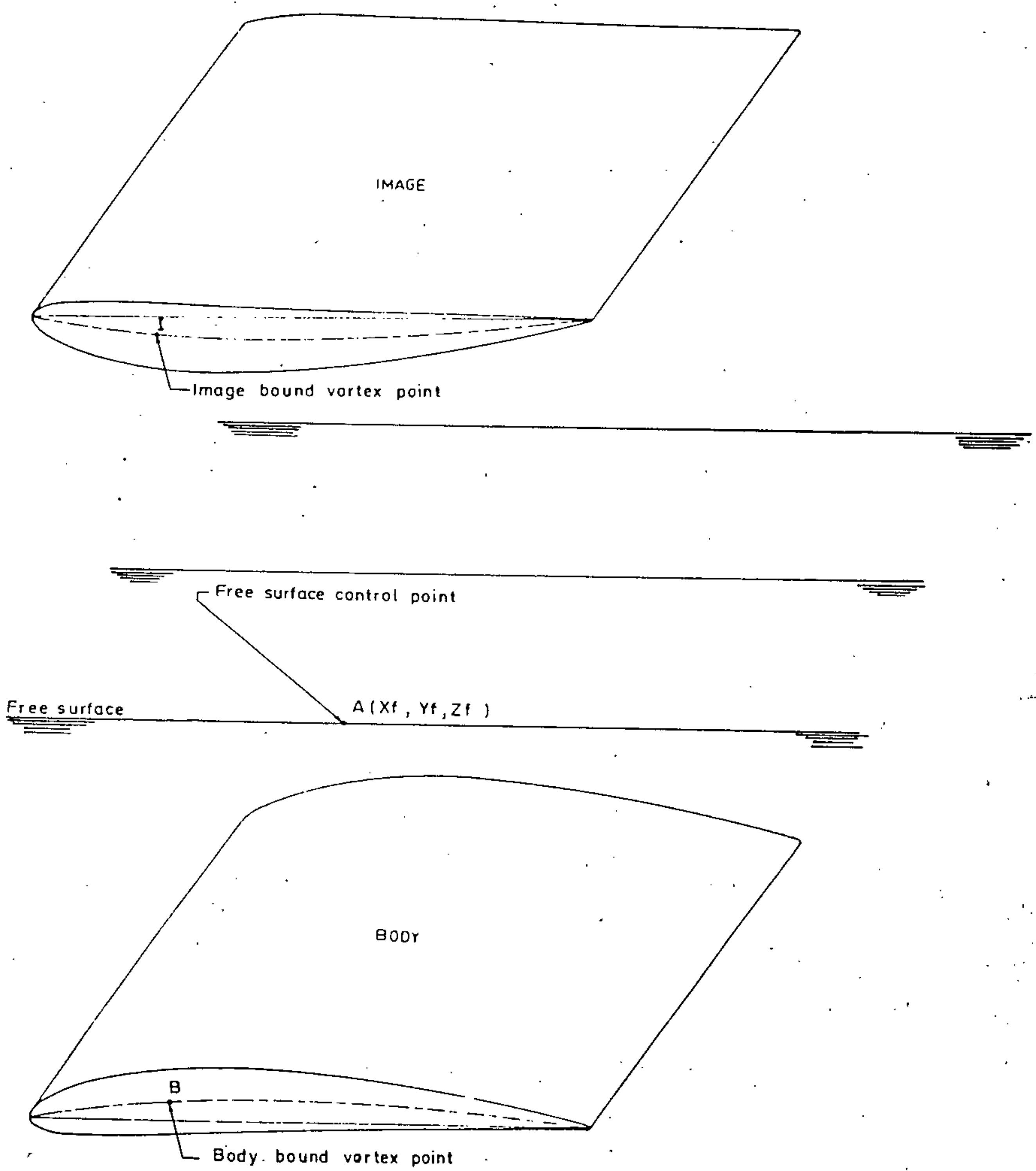

FIG. 3.5 : SHOWING A TYPICAL FREE SURFACE CONTROL POINT WHERE THE INDUCED VELOCITY IS CALCULATED DUE TO TYPICAL BODY AND IMAGE BOUND VORTEX ELEMENT.

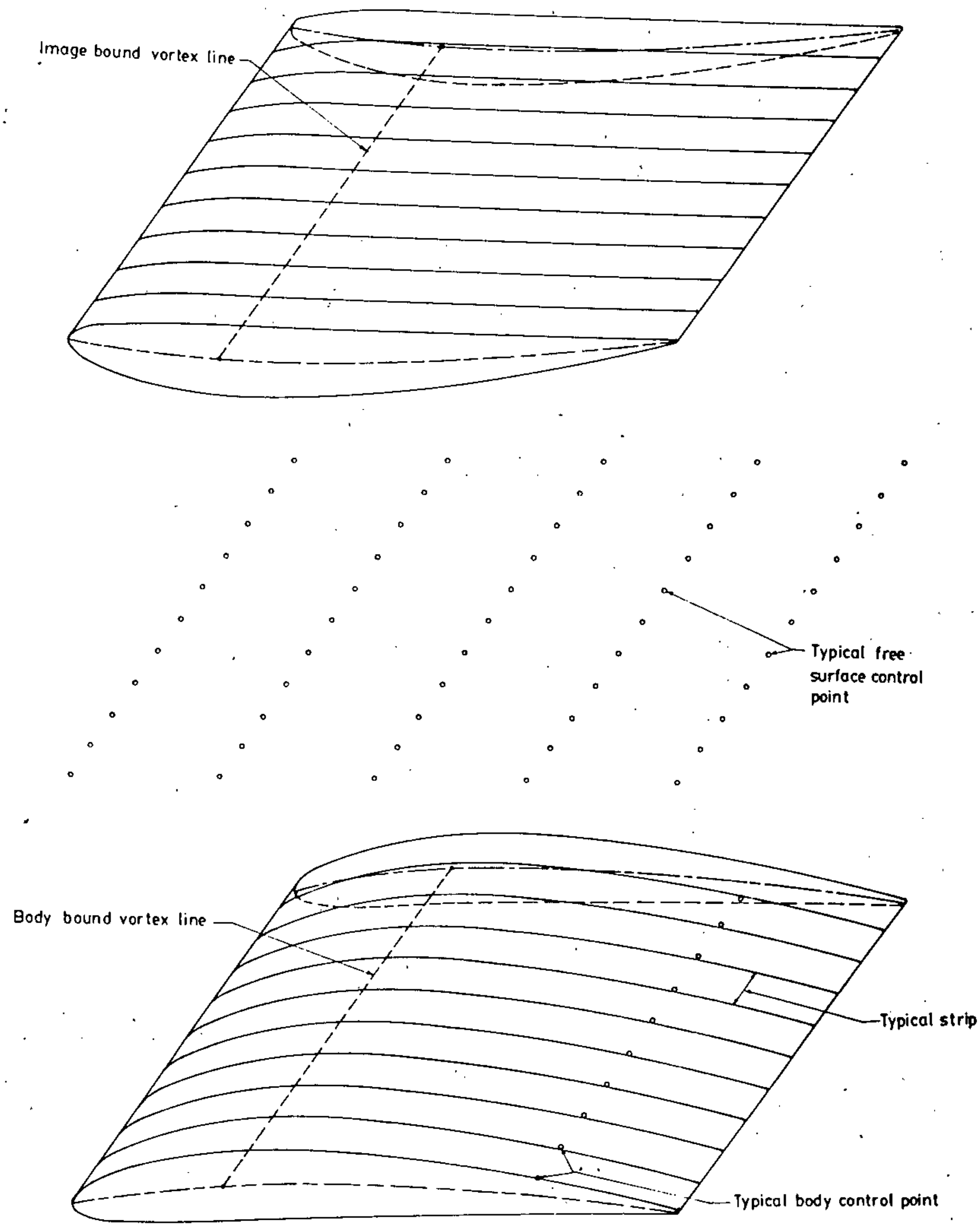

FIG. 3.6 BODY AND IMAGE OF A HYDROFOIL (CONSISTS OF TEN STRIPS ALONG SPAN) WITH UNDISTURBED FREE SURFACE

Where the influence coefficient $\vec{C}f,nb$ and $\vec{C}f,ni$ depend on the geometry of the nth horseshoe vortex and its image distance from the free surface control point. Since the governing equation is linear, the velocities induced by the 2N vortices are added together to obtain an expression for the total induced velocity at the mth control point which is .

$$\vec{V}f = \sum_{n=1}^{N} \Gamma n(\vec{C}f,nb + \vec{C}f,ni) \qquad \text{.............(3.16).}$$

CHAPTER - 4

EXPRESSIONS OF HYDROFOIL CHARACTERISTICS

4.0 SUMMARY OF THE CHAPTER

The formed circulation matrix using Biot-Savart law and vortex lattice method. is solved to satisffy the necessary boundary conditions to find circulation distribution .The induced velocity is then calculated at the hydrofoil control points . The induced velocity at free surface is also calculated to find the free surface deflection . The convergence of the free surface deflection rate is the image stabilizing criterion . Because the image will be stable, if the free surface is stable.After the convergence of the solution the calculation of different hydrofoil characteristics are carried out.

4.1. CALCULATION OF CIRCULATION DISTRIBUTION ON THE HYDROFOIL SURFACE

To calculate the induced velocity on the hydrofoil surface, circulation value is required. Equation(3.12) and (3.13) give the relation of circulation and inducd velocity. The right hand side of equation (3.13) possesses unknown circulation . Equation (2.4) forms N number of equations containing N number unknown circulation . Using Gauss-Seidel [11] method these equations are solved to find circulation.

4.2 VELOCITY CALCULATION

4.2.1 AT THE HYDROFOIL CONTROL POINT

At the hydrofoil control point the induced velocity can be written using equation (3.14) as

$$\vec{V}m = \sum_{n=1}^{N} \Gamma n(\vec{C}m,nb + \vec{C}m,ni) \quad \ldots\ldots\ldots\ldots(4.1)$$

where,

m stands hydrofoil control point

b stands body and

i stands image

4.2.2 AT THE FREE SURFACE

At any point of the free surface the induced velocity can be written using equation (3.16), as

$$\vec{V}f = \sum_{n=1}^{N} \Gamma n \quad (\vec{C}f,\ nb + \vec{C}f,\ ni) \quad \ldots\ldots\ldots\ldots\ldots\ldots(4.2)$$

where f stands free surface

b stands body and

i stands image.

4.3 CALCULATION OF LIFT, DRAG AND MOMENT COEFFICIENTS

LIFT COEFFICIENT

Using Kutta-Joukowski theorem to determine the lift force per unit span can be written as

$$L = \rho \, \Gamma_n \, (U_\infty + V_x) \quad \ldots\ldots (4.3)$$

To get total lift coefficient of that elemental section, equation (4.3) can be multiplied by the width of the section (dSn) which is equal to the span length divided by the number of strips.

So the section lift coefficient

$$dC_L = L \cdot dSn / (A \, \rho U_\infty^2) 1/2 \ldots\ldots (4.4)$$

where,

A is the area of the elemental section. With the help of equation (4.3), equation (4.4) can be written, as

$$dC_L = \rho \Gamma_n (U_\infty + V_x) dSn / \rho A U_\infty^2 \cdot 1/2$$

by rearranging it can be written as,

$$dC_L = 2 \Gamma_n (U_\infty + V_x) / C \cdot U_\infty^2 \quad \ldots\ldots (4.5)$$

The total lift coefficient of the hydrofoil is the arithmetic average of the summation of section lift coefficients.

i.e., $$C_L = \left(\sum_{n=1}^{N} dC_L \right) 1/Nstrip \quad \ldots\ldots\ldots(4.6)$$

DRAG COEFFICIENT :

The total drag force experienced by the hydrofoil is

$$D = \rho\, VZ\ \Gamma n\ dSn \quad \ldots\ldots\ldots\ldots\ldots(4.7)$$

The section drag coefficient

$$dC_D = D/(\rho A\, U_\infty^2/2) \quad \ldots\ldots\ldots(4.8)$$

yields,

$$dC_D = 2\rho VZ\ \Gamma ndSn/\ \rho\ dSn\ C\ U_\infty^2 \quad \ldots\ldots\ldots(4.9)$$

$$dC_D = 2VZ\,\Gamma n / C \cdot U_\infty^2$$

Arithmetic average of the summation of section drag coefficient gives the total drag coefficient. Mathematically.

$$C_D = 1/\text{Nstrip}\left(\sum_{n=1}^{N} dC_D n\right) \quad \ldots\ldots\ldots\ldots\ldots\ldots\ldots\ldots(4.11)$$

MOMENT COEFFICIENT :

Like lift and drag coefficient section moment coefficient is

$$dC_M = dC_L\ ((XMY - X1n)\ \cos\alpha\ -\ (Z1n - ZMY)\ \sin\alpha + dC_D\ ((Z1n - ZMY) \times \cos\alpha\ + (XMY-X1n)\ \sin\alpha \quad \ldots\ldots\ldots\ldots\ldots\ldots\ldots\ldots \quad (4.12)$$

where, XMX is X coordinate and ZMY is z coordinate at the mid point of the mean foil section.

To get the total moment coefficient, the summation of section moment coefficient is to be divided by the number of strips.

i.e., $$C_M = (1/\text{Nstrip})\left(\sum_{n=1}^{N} dC_M\right) \quad \ldots\ldots(4.13)$$

4.4 FREE SURFACE DEFLECTION CALCULATION :

The formed image with the hydrofoil and disturbed surface are shown in the Fig. 4.1.Applying Bernoulli's equation for steady flow on the surface Z = h, assuming is deflection of the disturbed surface.

$$\frac{P_\infty}{\rho} + [(U_\infty + Vx_s)^2 + V^2y_s + V^2z_s] + g(h + \varphi) = \frac{P_\infty}{\rho} + \frac{U_\infty^2}{2} + g.h \quad \cdots\cdots (4.14)$$

After rearrangement,to find it may be written as,

$$\varphi = -[U_\infty Vx_s + \tfrac{1}{2}(V^2x_s + V^2y_s + V^2z_s)]/g \quad \cdots\cdots (4.15)$$

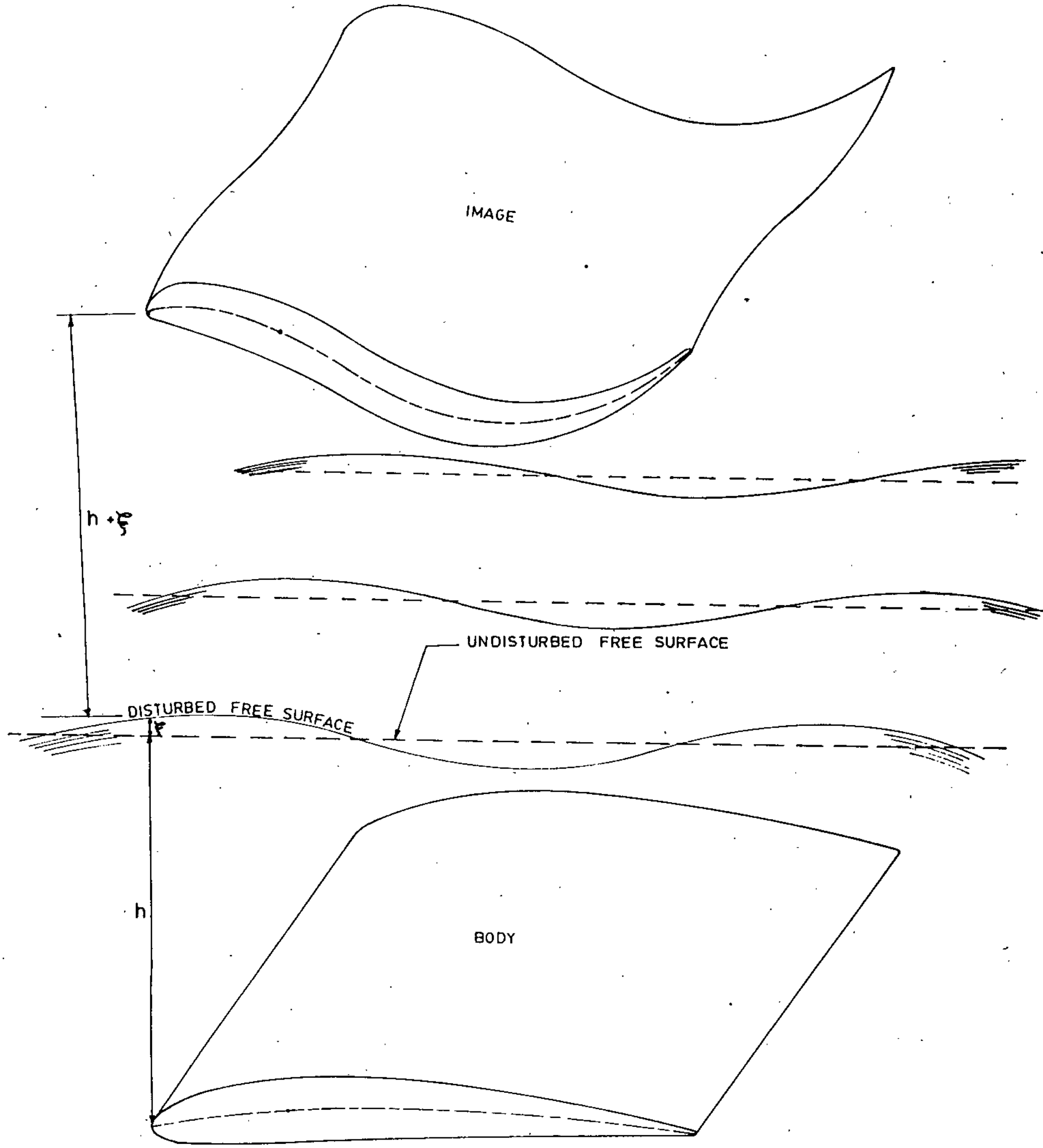

FIG. 4.1 : HYDROFOIL AND IMAGE WITH DISTURBED FREE SURFACE.

CHAPTER-5

COMPUTATION METHOD

5.0 SUMMARY OF THE CHAPTER

This chapter describes the calculation procedure using the theory developed and computer programming.Two section profiles are used for calculation given in Appendix [B] and [C].The calculation procedure is shown by computer programming flow chart.The required CPU time for various runs are given in Appendix [D].

5.1 CALCULATION METHOD

The flow chart of computer programing is shown in the next page. The Computer programme listing is provided in Appendix [A].

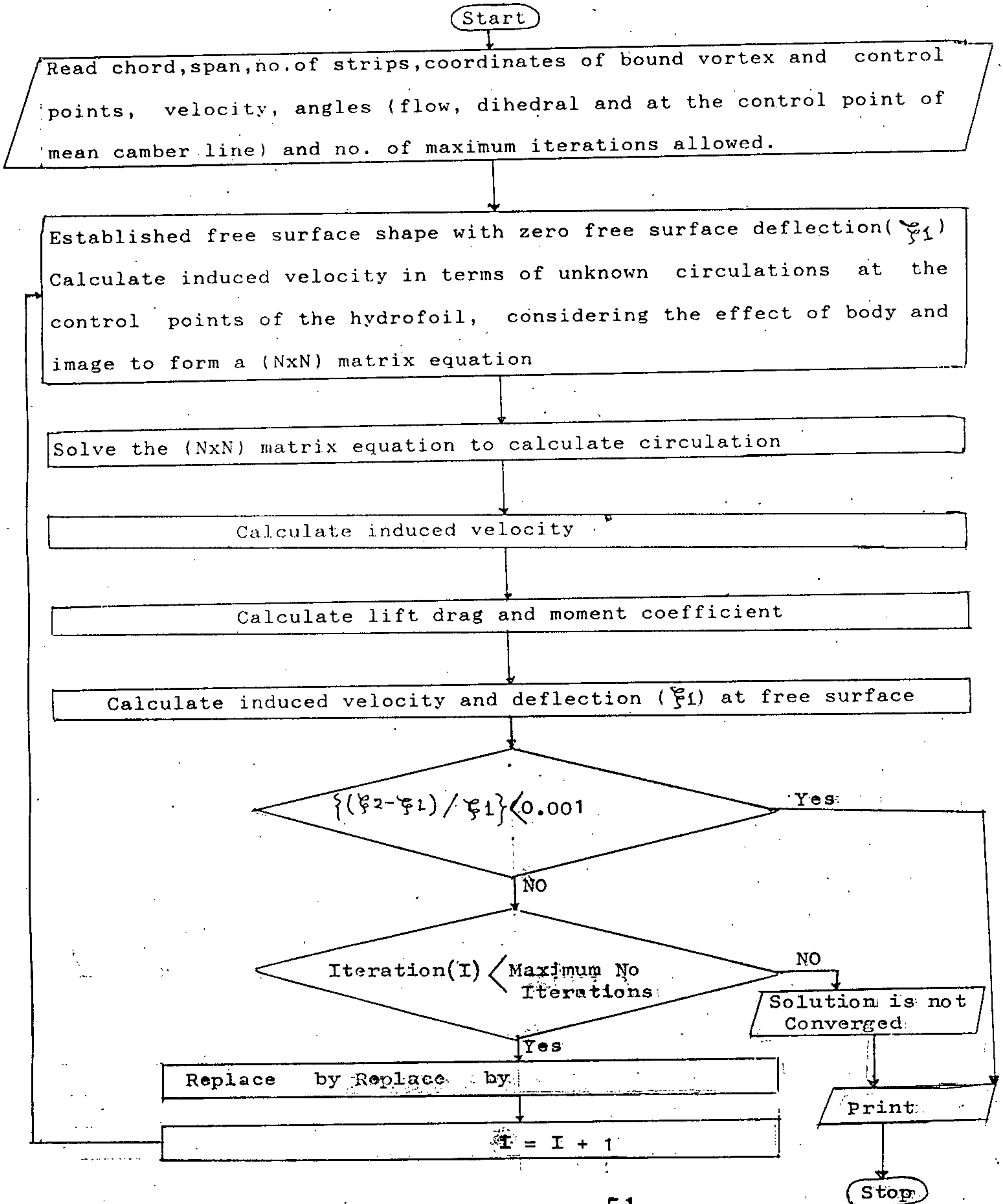

Computer programming flow chart.

5.2 PROFILE DATA USED

The acceptance of any developed theory lies with how it compares with available theoretical and experimental predictions. As some theoretical results related to NACA 4412 and NACA 16-206 [12] profile are available, these section profiles are chosen for present investigation. The related section profiles with offset data are given in Appendix [B] and [C].

5.3. PROGRAMME EXECUTION TIME

The calculation using present method developed is based on computer programming and the idea about the total programme execution time is required. For the present programme the execution time varies and depends on the number of iterations necessary to have the result. In Appendix [D] the virtual and total CPU time required for the programme execution is given for different number of iterations.

CHAPTER-6

RESULTS AND DISCUSSIONS

6.0 SUMMARY OF THE CHAPTER

To validate the theory developed the obtained results using theory developed should be compared with different available results. For comparisons the available theoretical results and obtained results for NACA 4412 are given in Table 6.1 to 6.6 & Figure 6.3 to 6.5. The results of NACA 16-206 are given in Table 6.7 to 6.10.

6.1 PRESENTATION OF CALCULATED RESULTS

6.1.1 WITH NACA 4412 PROFILE DATA

The comparisons of different hydrofoil characteristics calculated using existing theory and theory developed for NACA 4412 section profile are given in Table 6.1 to 6.6. The comparison in graphical form are shown in Figure 6.3 to 6.5. In Fig. 6.3 it is seen that the existing theoretical results [Ref. 13] are for infinite aspect ratio (i.e., 2-Dimensional). But the results of theory developed are for finite aspect ratio (i.e. 3-Dimensional). From this Figure it is seen that, lift coeficient increases with the increment of aspect ratio. So, the variation of lift coefficient between the existing theory and the theory developed may be acceptable.

Figure 6.2 and 6.3 show the comparison in ratio of lift coefficient (with free surface to without free surface), with variation in aspect ratio and Froude number (Fr*). From Fig 6.2 for aspect ratio five it is seen that as the Froude No.(Fr.*) increases, the variation between the two theories decreases and at Froude No.(Fr*)= 2.236, the two theories compares very close. From Figure 6.3 for aspect ratio eight , it is seen that as the Froude No. (Fr*) increases the variaion between the two theories decreases and at Froude No. (Fr.*) = 2, the two theories again compares very close.

Figure 6.4 shows the variation of lift coefficient with the variation of Froude Number (Fr*) .From this curve it is seen that abrupt variation occurs between the range of Froude Number (Fr*) one and two .The change of lift coefficient within Froude Number (Fr*) one is very small. The same Figure shows the variation with aspect ratio eight. The pattern of the two curves is similar.But for aspect ratio eight the variation of lift coefficient within Froude Number (Fr*) one is relatively large than that of aspect ratio five.

Table 6.1 : Lift,drag and moment coefficient of NACA 4412 with

$\lambda = 5$, C=1, h=1, Fr*=1, $\phi = 0$

Image condition	Flow condition	Lift coefficient	Drag coefficient	Moment coefficient
with	$\alpha = 0$	0.33562	-0.0303236	0.835254
without		0.3785	-0.0344089	0.0947781
with	$\alpha = 5$	0.645765	-0.115881	0.159066
without		0.739268	-0.131499	0.182118
with	$\alpha = 10$	0.947029	-0.254097	0.223975
without		1.09378	-0.28837	0.25888

Table - 6.2 : Lift,drag and moment coefficient of NACA 4412 with aspect ratio 5 , unit chord and zero angle of attack and dihedral

Image condition	Flow Condition	Froude number(Fr)*	lift coefficient C_L	Drag coefficient C_D	Moment coefficient C_M
with	h = 20	0.5	0.378264	-0.0343873	0.0947191
	h = 5	1	0.374828	-0.0340750	0.0938586
with	h = 1.25	2	0.344173	-0.312882	0.0861824
	h = 1	2.236	0.333537	-0.0303212	0.0835191
without			0.3785	-0.0344088	0.0947481

Table - 6.3: Lift, drag and moment coefficient of NACA 4412 with aspect ratio 8, unit chord and zero angle of attack.

Image Condition	Flow Condition		Froude Number	Lift coeffi-	Drag coefficient	Moment coefficient
Without		$\varphi=0$	0.5	0.437083	-0.0397344	0.109489
		$\varphi=30$		0.437077	-0.0397338	0.109444
	h=20	$\varphi=0$		0.436585	-0.0397892	0.109321
		$\varphi=30$		0.436579	-0.0396886	0.109321
with	h=5	$\varphi=0$	1	0.430207	-0.0391079	0.107722
		$\varphi=30$		0.430191	-0.039108	0.10772
	h=1.25	$\varphi=0$	2	0.392056	-0.0356411	0.0981708
		$\varphi=30$		0.391715	-0.0356101	0.0980853
	h=1.0	$\varphi=0$	2.236	0.380201	-0.0345209	0.0952024
		$\varphi=30$		0.379733	-0.0345208	0.0950851

Table - 6.4 : Variation in lift coefficient ratio of NACA 4412 with variation of Froude number (Fr*) and dihedral angle for aspect ratio 8.

Flow condition(Fr*)	Dihedral angle	$C_L/C_{L\infty}$
0.5	0	0.9988606
	30	0.9988606
1.0	0	0.9885307
	30	0.9842453
2.0	0	0.8969829
	30	0.8962150
2.236	0	0.8698599
	30	0.8688011

Table -6.5 : Ratio of lift coefficient of NACA 4412 with aspect ratio 8 with the variation of Froude number (Fr*) and zero angle of attack'.

Flow condition (Fr*)	Image condition	$C_L(0)/C_L(30)$ (*)
0.5	Without	1.0000137
	With	1.0000137
1.0	With	1.0000372
2.0	With	1.00008705
2.236	With	1.0012324

* 0 stands for dihedral =0

30 stands for dihedral =30

Table - 6.6 : Comparison of lift, drag and moment coefficient of NACA 4412 with the variation of depth of submergence and numebr of strips with zero angle of attack and dihedral for aspect ratio 5.

Depth of submer-gences	Number of strip	Froude No. (Fr*)	Lift coefficient CL	Drag coefficient CD	Moment coeffi-cient CM
1.0	4	2.236	0.355288	-0.0322986	0.088965
	8		0.337859	-0.0307142	0.0846015
	10		0.333537	-0.0303212	0.0835191
	12		0.330525	-0.0300477	0.0827966
5	4	1.0	0.400992	-0.0364535	0.100410
	8		0.37993	-0.0345389	0.0951363
	10		0.374828	-0.0340750	0.0938586
	12		0.37123	-0.033748	0.0929576

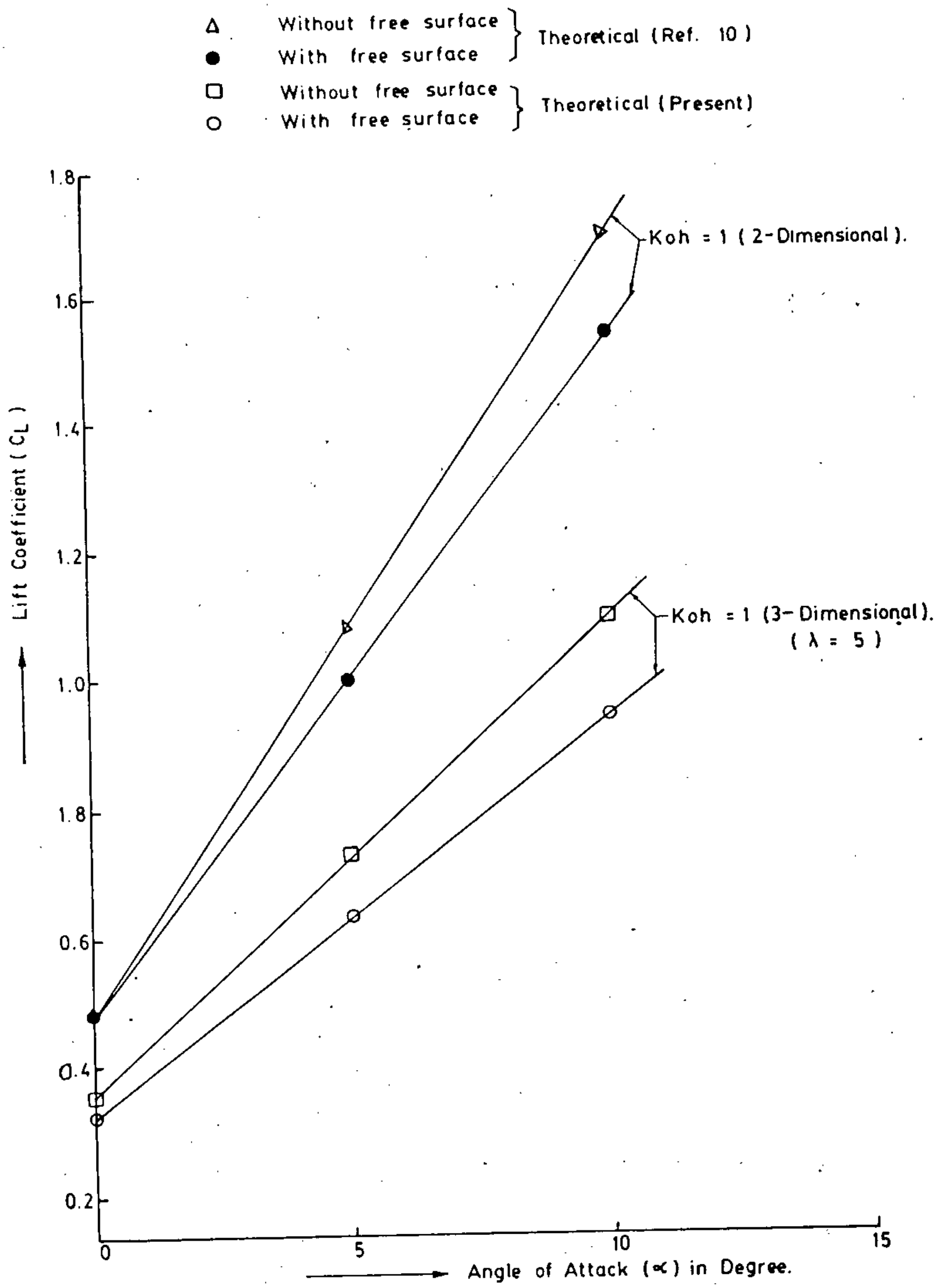

FIG. 6.1 COMPARISON OF LIFT COEFFICIENT WITH c/h = 1 for NACA 4412.

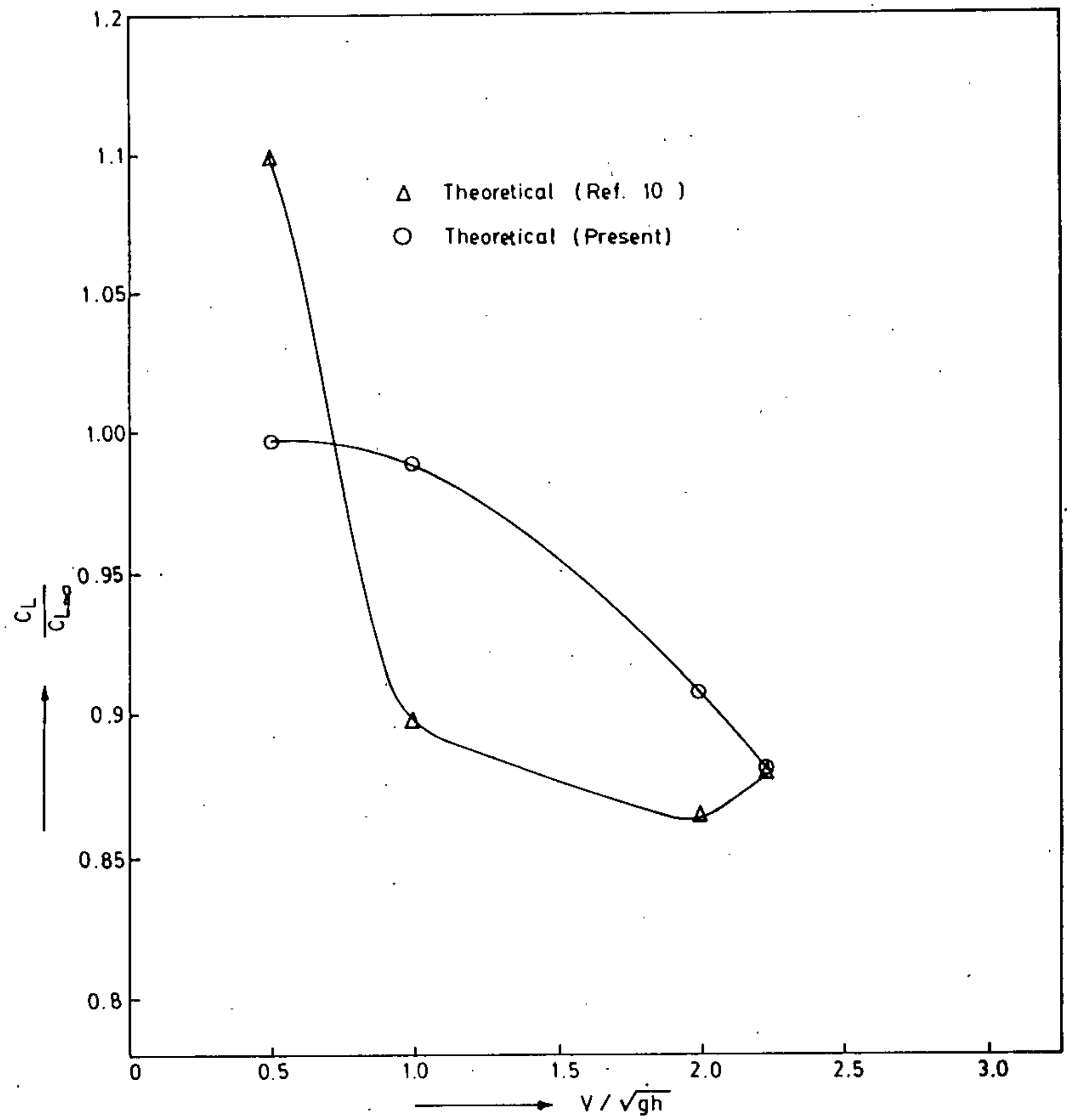

FIG. 6.2 : COMPARISON OF THE RATIO OF LIFT COEFFICIENT WITH THE FREE SURFACE TO WITHOUT FREE SURFACE FOR $\lambda = 5$ AND NACA 4412.

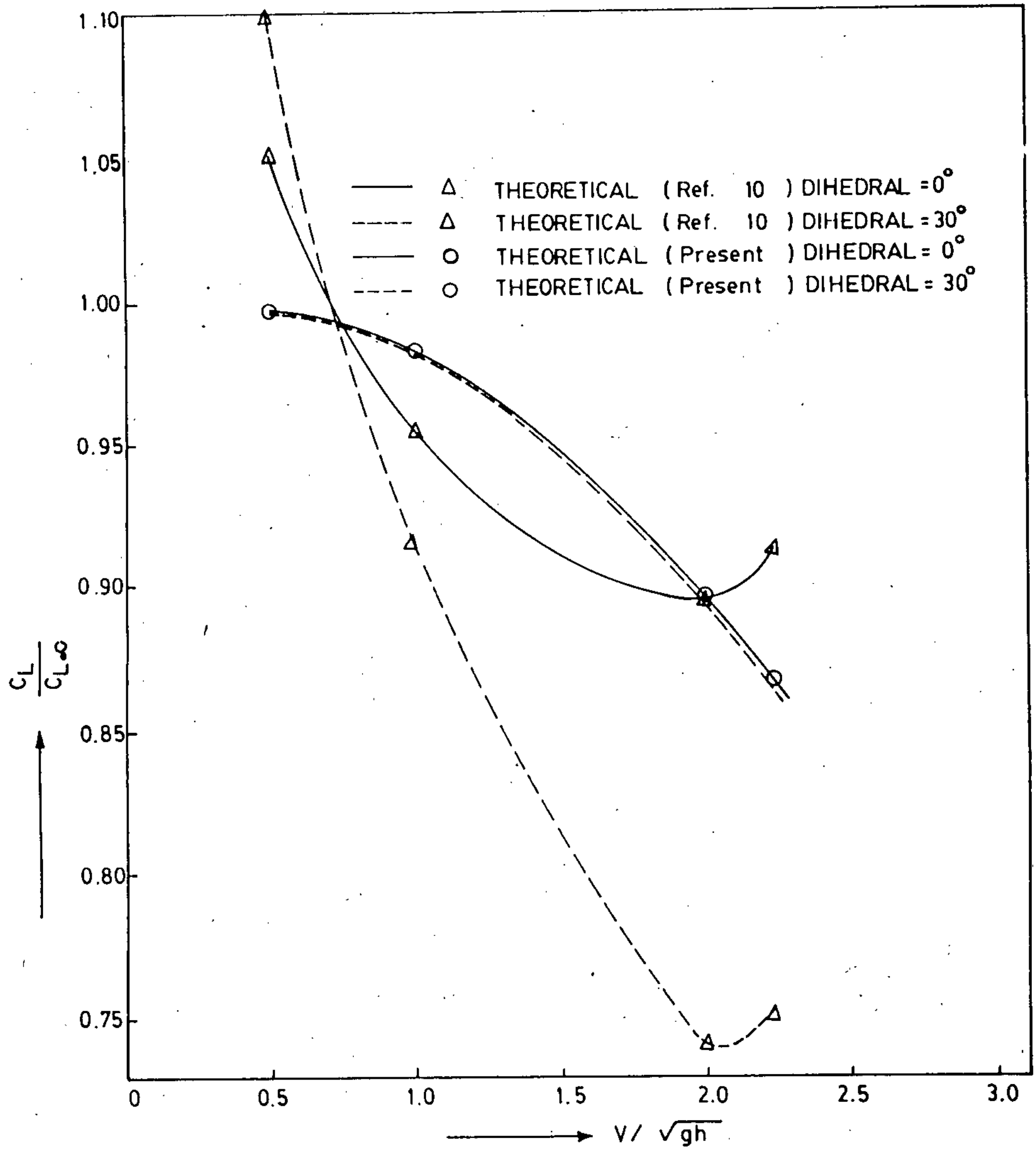

72260

FIG. 6.3 : COMPARISON OF THE RATIO OF LIFT COEFFICIENT WITH THE FREE SURFACE TO WITHOUT FREE SURFACE FOR $\lambda = 8$ AND NACA 4412 .

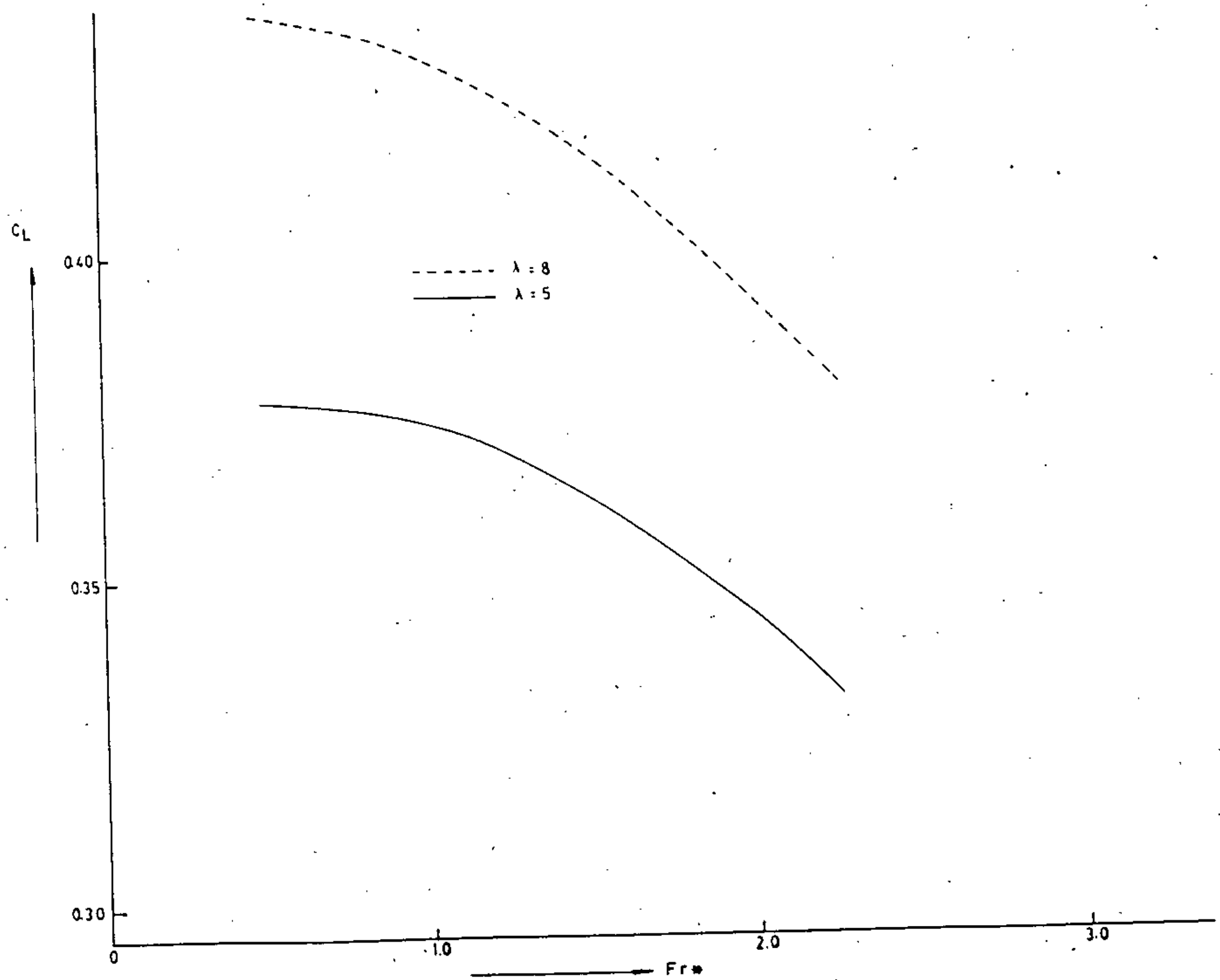

FIG. 6.4 VARIATION OF LIFT COEFFICIENT WITH THE VARIATION OF FROUDE NUMBER (Fr*), ASPECT RATIO, C = 1, $\alpha = 0$ AND $\Phi = 0$ OF NACA 4412

64

6.1.2. WITH NACA 16-206 PROFILE DATA

The different hydrofoil charactristics calculated using NACA 16-206 section profile are given in Table 6.7 to 6.10. Table 6.7 shows the variation of lift, drag and moment coefficient with aspect ratio. It is seen that as the aspect ratio increases the lift coefficient increases and if the aspect ratio increases six times, the lift coefficient increases near about two & half times. Table 6.8 shows the ratio of lift coefficient (with free surface to without free surface). From this table it is seen that as the aspect ratio increases six times, the ratio decreases near about twelve percent.This is because the rate of increment of lift coefficient without free surface is more than that of with free surface with the increment of aspect ratio). Table 6.9 shows the spanwise distribution of circulation with the variation of aspect ratio. From this table it can be seen that the circulation is maximum at the mid span and minimum at the end span and the variation is smooth. The same pattern follows for all types of aspect ratio. The spanwise variation in magnitude of circulation occurs with variation in aspect ratio and the increase in circulation occurs due to increase in aspect ratio. Table 6.10 shows the chordwise variation in distribution of free surface height at the midspan. Figure 5.6 shows the graphical form of Table 6.10 for different aspect ratios.For convinence of plotting Table 6.10 with non-dimensional form is given in Figure 5.7

Table 6.7 : Variation of lift, drag and moment coefficient of NACA 16- 206 with variation of aspect ratio and C = 1, h = 1, α = 0 and Fr*=4.6

Image condition	Aspect ratio	Lift Coefficient	Drag Coefficient	Moment Coefficient
Without	1.3333	0.0441226	-0.000990256	0.0110328
	5	0.0935867	-0.0021004	0.0234013
	8	0.10812	-0.00242658	0.0270352
With	1.3333	0.0426558	-0.000957338	0.010666
	5	0.0838583	-0.00188206	0.0209687
	8	0.096029	-0.00215522	0.024012

Table - 6.8 : Variation of lift Coefficient of NACA 16-206 with variation of aspect ratio and C= 1, h=1, α = 0, and Fr* = 4.6

Ratio of lift coefficient	Aspect ratio (λ)		
	1.3333	5	8
$C_L/C_{L\infty}$	.9667562	.8960493	.8881705

Table - 6.9 : Variation of circulation along span of NACA 16-206 with variation of aspect ratio.

Strip number along span	$\lambda = 1.3333$	$\lambda = 5$	$\lambda = 8$
	Circulation		
1	.199800	.447861	.552617
2	.281654	.582916	.680241
3	.329216	.642695	.728126
4	.356857	.671044	.749609
5	.369724	.682713	.758444
6	.369718	.682713	.758444
7	.356843	.671044	.749609
8	.329172	.642694	.728127
9	.281596	.582914	.680241
10	.199760	.447861	.552618

Table - 6.10 : Comparison of chordwise variation of the disturbed free surface height at the midspan of NACA 16-206 with variation of aspect ratio.

	Leading Edge	25% of chord Location	50% of chord Location	75% of chord Location	Trailing Edge
1.33	-.2749E-04	-.129721E-03	-.293871E-03	-.433003E-03	-.50906E-03
5	.66262E-04	-.360079E-03	-.122112E-02	-.186070E-02	-.21243E-02
8	.88703E-04	-.202188E-03	-.102205E-02	-.165187E-02	-.18929E-02

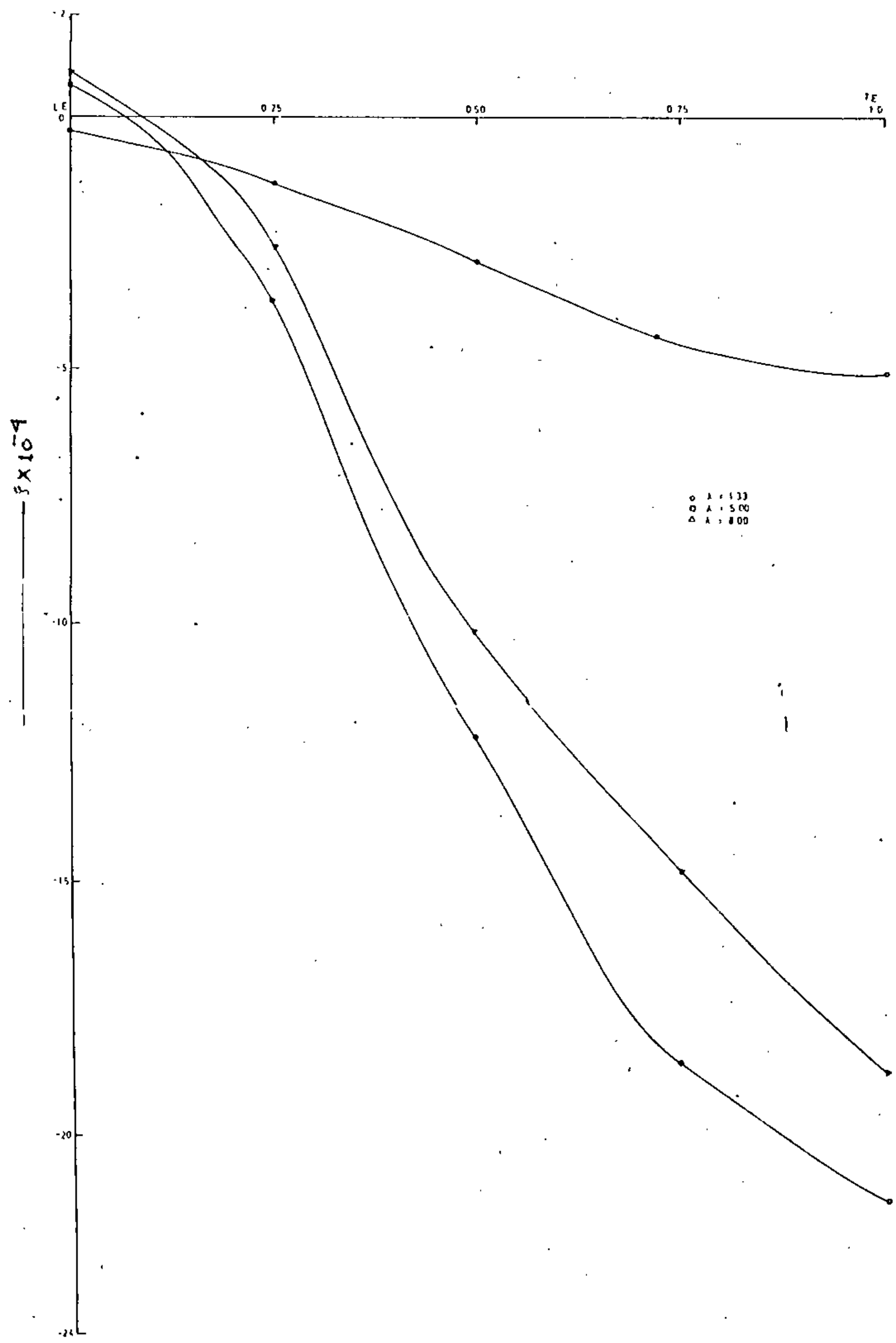

FIG 6.5 CHORDWISE VARIATION OF DISTURBED FREE SURFACE HEIGHT AT THE MIDSPAN OF NACA 16-206 WITH VARIATION OF ASPECT RATIO

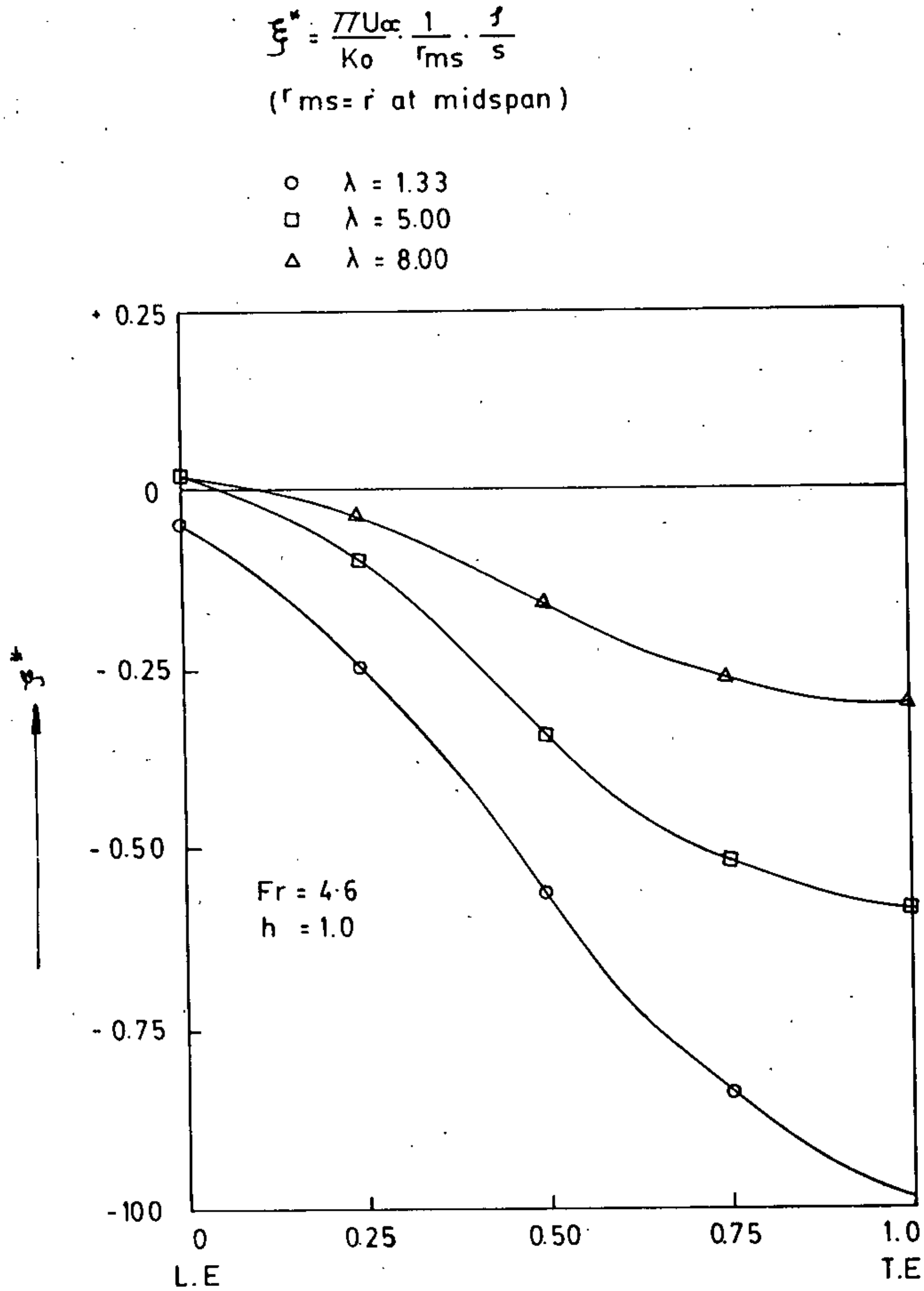

FIG. 6.6 VARIATION OF ξ^* WITH THE VARIATION OF ASPECT RATIO OF NACA 16-206 (AT THE MIDSPAN)

CHAPTER-7

CONCLUSIONS AND RECOMMENDATIONS

7.1 CONCLUSIONS

The present method developed the computaional procedure includes use of Biot-Savart Law for the calculation of induced velocity, vortex lattice method is used to approximate the hydrofoil and image stabilizing criterion is used for the convergence of the solution. Image stabilizing criterion also stablized the free water surface. In vortex lattice method the number of strips into which the hydrofil to be divided bears some importance in the accuracy of the predicted result. In the present calculation the number of strips are taken as ten for all calculations and all the strips are of equal width. If the numebr of strips are relatively small, error arises in predicted hydrofoil characteristics and usually predicts less. Again due to end effect the given convergence criterion does not satisfy for more number of strips. For the difficulty arises in satisfing this convergence criterion many existing methods use the first solution without performing any convergence test.

The method developed is used to predict differnt characteristics of hydrofoils with variation in geometry and operation. As the theoretical results of NACA 4412 are available, so this section profile is used for comparison with different aspect ratio, such as five and eight. The comparison gives good results. Another section profile such as NACA 16-206 is used for prediction of different charactristics with different aspect ratio such as four by three, five and eight . In one case the later section profile is used for a relatively small aspect ratio such as 4/3. This is done to observe the foil characteristics of nearly squared shape.

The developed computer programme has some limitations. The main drawback is in satisfying the given convergence criterion. The given convergence criterion does not satisfy for very high Froude number (Fr*) because in very high Froude number (Fr*) the depth of submergence is comparatively very low and the disturbed free surface height is relatively large.

7.2 RECOMMENDATIONS

Followings are the recommendations for future work regarding the prediction of hydrofoil characteristics.

The detailed flow field near the hydrofoil can be predicted with proper extension of the calculation. The method developed can be extended for exact lifting surface and lifting body solution with proper modifications.

REFERENCES

1. Brian Russell,'Hydrofoil', Small ships, Chris wilbur, January / February, 1983.

2. Hatch G.N. , 'Creative Naval Architecture', K.D. Troup,1971.

3. Thomas C. Gillmer & Bruce Johnson, 'Introduction to Naval Architecture', E.& F.N. spon Ltd., 1982.

4. F.H.Todd,'chapter Vll- Resistance and Propulsion',Principles of Naval Architecture,John.P.Comstrck,Society of Naval Architecture and Marine Engineers,Newyork,1967.

5. Robertson, J.M.'Hydrodynamics in theory and application',1965

6. Solvesen, N., 'On Higher-order theory for submerged two-dimensioal bodies, Journal of Fluid Mechanics, Vol. 38, No.2, 1969.

7. Daniel K. ai, 'The detailed flow field near a hydrofoil of finite span at shallow submergences", Topics in ocean Engineering, charles J. Bretschneider, Gulf Publishing Company, 1969.

8. Joseph P. Geising and A.M.O. Smith, 'Potential flow about two - dimensional hydrofoils', Journal of Fluid Mechanics, Vol. 28, NO.1, 1967.

9. Clancy, L.J., 'Aerodynamics', Sir Isaac Pitman and Sons Ltd. (Great Britan), 1975.

10. John J. Bertin & Michael .Smith, 'Aerodynamics for Engineers', Prentice Hall Inc. U.S.A. 1979.

11. James B. Scarborough, 'Numerical Mathematical Analysis', 6th edition, Oxford and IBH Publishing Co. Ltd., 1966.

12. Ira H.Abbott & Albert E.Von Doenhoff,'Theory of wing sections', Dover publications,Inc,New York,1959.

13. Tefsuo Nishiyama, 'study on submerged Hydrofoils', 60th Anniversary series, The society of Naval Architects of Japan, Volume 2, 1972.

APPENDICES

```
C     ------------------------------------------------------------------
C     X-AXIS IS ALONG CHORDWISE
C     Y-AXIS IS ALONG SPANWISE
C     Z-AXIS IS ALONG CHORD HIGHETWISE
C     ANGLES ARE TAKEN IN DEGREE AND MEASURED ANTICLOCKWISE POSITIVE
C     BOUND VORTEX POINTS ARE TAKEN AT 25 PERCENT OF CHORD LENGTH
C     CONTROL POINTS ARE TAKEN AT 75 PERCENT OF CHORD LENGTH
C     XBC,YBC,ZBC ARE THE CO-ORDINATES OF BODY CONTROL POINTS
C     X1,Y1,Z1 ARE THE CO-ORDINATES OF BOUND VORTEX POINTS AT THE
C     FIRST CORNER
C     X2,Y2,Z2 ARE THE CO-ORDINATES OF BOUND VORTEX POINTS AT THE
C     SECOND CORNER
C     XMY IS THE X-COORDINATE OF THE MOMENT AXIS
C     ZMY IS THE Z-COORDINATE OF THE MOMENT AXIS
C     MITER IS THE MAXIMUM NUMBER OF ITERATIONS ALLOWED
C     NSTRIP REPRESENTS THE NUMBER OF STRIP TAKEN ALONG SPANWISE
C     NUMBER OF STRIP WILL BE MAXIMUM FIFTEEN(15) FOR THIS READY
C     PROGRAM. IF NUMBER OF STRIP IS MORE THAN 15 THEN DIMENSION
C     SHOULD BE CHANGED ACCORDING TO NUMBER OF STRIP
C     FVELOC REPRESENTS THE SPEED OF FLOW
C     FANGLE REPRESENTS THE ANGLE OF ATTACK
C     DANGLE REPRESENTS THE DIHEDRAL ANGLE
C     CANGLE REPRESENTS THE SLOPE OF MEAN CAMBER LINE AT CONTROL POINT
C     DEPTH REPRESENTS THE DEPTH OF SUBMERGENCE OF THE FOIL
C     ------------------------------------------------------------------
      DIMENSION XBC(15),YBC(15),ZBC(15),
     #XB1(15),YB1(15),ZB1(15),XB2(15),YB2(15),ZB2(15),
     #X(16),Y(16),Z(16),X1(16),Y1(16),Z1(16),
     #X2(16),Y2(16),Z2(16),C(16,16),D(16,16),E(16,16),F(16,16),
     #G(16,16),H(16,16),P(16,16),Q(16,16),R(16,16),S(16,16),T(16,16),
     #CC(16,16),DD(16,16),A(16,16),U(16,16),V(16,16),W(16,16),B(16),
     #X3(16),VX1(16,16),VY1(16,16),VZ1(16,16),
     #VX2(16),VY2(16),VZ2(16),XF(16,5),YF(16,5),ZF(16,5),
     #VXS(16,5),VYS(16,5),VZS(16,5),ZCI(16,5),ZCIL(16),DZCI(16)
C     ------------------------------------------------------------------
C     READ DATA FROM UNIT 2
C     ------------------------------------------------------------------
      OPEN(UNIT=2,FILE='IN',STATUS='OLD')
      OPEN(UNIT=9,FILE='OUT',STATUS='NEW')
      READ(2,10)CHORD,SPAN
      READ(2,11)NSTRIP
      DO 51 I=1,NSTRIP
      READ(2,12)XBC(I),YBC(I),ZBC(I),XB1(I),YB1(I),
     #ZB1(I),XB2(I),YB2(I),ZB2(I)
   51 CONTINUE
      READ(2,13)FVELOC,FANGLE,DANGLE,CANGLE,DEPTH
      READ(2,33)XMY,ZMY
      READ(2,37)MITER
C     ------------------------------------------------------------------
C     WRITE DATA IN UNIT 9
C     ------------------------------------------------------------------
      WRITE(9,14)
      WRITE(9,15)CHORD,SPAN
      WRITE(9,16)NSTRIP
      WRITE(9,17)
```

```
      DO 52 J=1,NSTRIP
      WRITE(9,18)J,XBC(J),YBC(J),ZBC(J),XB1(J),YB1(J),
     #ZB1(J),XB2(J),YB2(J),ZB2(J)
   52 CONTINUE
      WRITE(9,19)FVELOC,FANGLE,DANGLE,CANGLE,DEPTH
      WRITE(9,34)XMY,ZMY
      WRITE(9,38)MITER
C     ---------------------------------------------------------------
C     WRITE RESULTS IN UNIT 9
C     ---------------------------------------------------------------
      WRITE(9,20)
      PI=4.0*ATAN(1.0)
      NSF=NSTRIP+1
C     ---------------------------------------------------------------
C     FREE SURFACE SHAPE INITIALIZATION
C     ZCI REPRESENTS ZETA WHICH IS THE DEFLECTION OF FREE SURFACE
C     AS A FIRST APPROXIMATION ZCI=0.0
C     ---------------------------------------------------------------
      DO 68 M=1,NSF
      DO 69 N=1,5
      J=N-1
      JJ=M-1
      ZCI(M,N)=0.0
      XF(M,N)=0.25*CHORD*FLOAT(J)
      YF(M,N)=(SPAN/FLOAT(NSTRIP))*FLOAT(JJ)
      ZF(M,N)=DEPTH+ZCI(M,N)
   69 CONTINUE
   68 CONTINUE
      WRITE(9,22)((XF(M,N),N=1,5),M=1,NSF)
      WRITE(9,30)((YF(M,N),N=1,5),M=1,NSF)
      WRITE(9,31)((ZF(M,N),N=1,5),M=1,NSF)
C     ---------------------------------------------------------------
C     IZ IS THE NUMBER OF ITERATIONS REQUIRED FOR STABILIZING
C     THE IMAGE
C     ---------------------------------------------------------------
      DO 55 IZ=1,MITER
      WRITE(9,36)IZ
C     ---------------------------------------------------------------
C     CALCULATION OF INDUCED VELOCITY AT THE BODY CONTROL POINTS
C     DUE TO BODY AND IMAGE FOR UNKNOWN CIRCULATION
C     NI=1 FOR BODY
C     NI=2 FOR IMAGE
C     ---------------------------------------------------------------
      DO 56 M=1,NSTRIP
      DO 57 N=1,NSTRIP
      VX1(M,N)=0.0
      VY1(M,N)=0.0
      VZ1(M,N)=0.0
      A(M,N)=0.0
   57 CONTINUE
   56 CONTINUE
      DO 58 M=1,NSTRIP
      X(M)=XBC(M)
      Y(M)=YBC(M)
      Z(M)=ZBC(M)
```

```
      DO 59 N=1,NSTRIP
      X1(N)=XB1(N)
      Y1(N)=YB1(N)
      X2(N)=XB2(N)
      Y2(N)=YB2(N)
      DO 60 N1=1,2
      IF(N1.EQ.2)GO TO 61
      Z1(N)=ZB1(N)
      Z2(N)=ZB2(N)
      GO TO 62
 61   Z1(N)=2.0*(DEPTH+ZCI(N,2))-ZB1(N)
      Z2(N)=2.0*(DEPTH+ZCI(N+1,2))-ZB2(N)
 62   C(M,N)=((Y(M)-Y1(N))*(Z(M)-Z2(N)))-((Y(M)-Y2(N))*(Z(M)-Z1(N)))
      D(M,N)=((X(M)-X1(N))*(Z(M)-Z2(N)))-((X(M)-X2(N))*(Z(M)-Z1(N)))
      E(M,N)=((X(M)-X1(N))*(Y(M)-Y2(N)))-((X(M)-X2(N))*(Y(M)-Y1(N)))
      F(M,N)=(X2(N)-X1(N))*(X(M)-X1(N))+(Y2(N)-Y1(N))*(Y(M)-Y1(N))+
     #(Z2(N)-Z1(N))*(Z(M)-Z1(N))
      G(M,N)=(X2(N)-X1(N))*(X(M)-X2(N))+(Y2(N)-Y1(N))*(Y(M)-Y2(N))+
     #(Z2(N)-Z1(N))*(Z(M)-Z2(N))
      H(M,N)=SQRT((X(M)-X1(N))**2+(Y(M)-Y1(N))**2+(Z(M)-Z1(N))**2)
      P(M,N)=SQRT((X(M)-X2(N))**2+(Y(M)-Y2(N))**2+(Z(M)-Z2(N))**2)
      Q(M,N)=(Z(M)-Z1(N))**2+(Y1(N)-Y(M))**2
      R(M,N)=(Z(M)-Z2(N))**2+(Y2(N)-Y(M))**2
      S(M,N)=(F(M,N)/H(M,N))-(G(M,N)/P(M,N))
      T(M,N)=C(M,N)*C(M,N)+D(M,N)*D(M,N)+E(M,N)*E(M,N)
      CC(M,N)=((Z(M)-Z1(N))/Q(M,N))*(1.0+((X(M)-X1(N))/H(M,N)))-
     #((Z(M)-Z2(N))/R(M,N))*(1.0+((X(M)-X1(N))/P(M,N)))
      DD(M,N)=((Y1(N)-Y(M))/Q(M,N))*(1.0+((X(M)-X1(N))/H(M,N)))-
     #((Y2(N)-Y(M))/R(M,N))*(1.0+((X(M)-X2(N))/P(M,N)))
      U(M,N)=(C(M,N)*S(M,N)/T(M,N))/(4.0*PI)
      V(M,N)=(CC(M,N)-((D(M,N)*S(M,N))/T(M,N)))/(4.0*PI)
      W(M,N)=((E(M,N)*S(M,N)/T(M,N))+DD(M,N))/(4.0*PI)
      VX1(M,N)=VX1(M,N)+U(M,N)
      VY1(M,N)=VY1(M,N)+V(M,N)
      VZ1(M,N)=VZ1(M,N)+W(M,N)
      A(M,N)=A(M,N)+(((U(M,N)*SIN(CANGLE*PI/180.0))
     #+(V(M,N)*COS(CANGLE*PI/180.0)*TAN(DANGLE*PI/180.0))
     #-(W(M,N)*COS(CANGLE*PI/180.0)))/(SIN((FANGLE-CANGLE)*PI/180.0)))
 60   CONTINUE
 59   CONTINUE
 58   CONTINUE
      WRITE(9,21)((A(M,N),N=1,NSTRIP),M=1,NSTRIP)
      DO 63 I=1,NSTRIP
      B(I)=FVELOC
 63   CONTINUE
      WRITE(9,22)(B(I),I=1,NSTRIP)
C     ------------------------------------------------------------------
C     CALCULATION OF CIRCULATION SOLVING REQUIRED MATRIX EQUATION
C     ------------------------------------------------------------------
      M=NSTRIP
      CALL SOLVE(A,B,M,X3)
      WRITE(9,23)
      DO 64 I=1,NSTRIP
      WRITE(9,24)I,X3(I)
 64   CONTINUE
```

```fortran
C     ----------------------------------------------------------------
C     CALCULATION OF LIFT, DRAG AND MOMENT COEFFICIENTS
C     AND INDUCED VELOCITY CALCULATION AT BODY CONTROL POINTS
C     ----------------------------------------------------------------
      CL=0.0
      CD=0.0
      CM=0.0
      WRITE(9,25)
      DO 65 M=1,NSTRIP
      VX2(M)=0.0
      VY2(M)=0.0
      VZ2(M)=0.0
      DO 66 N=1,NSTRIP
      VX2(M)=VX2(M)+X3(N)*VX1(M,N)
      VY2(M)=VY2(M)+X3(N)*VY1(M,N)
      VZ2(M)=VZ2(M)+X3(N)*VZ1(M,N)
   66 CONTINUE
      CLY=(2.0*(FVELOC+VX2(M))*X3(M))/(CHORD*FVELOC*FVELOC)
      CDY=(2.0*VZ2(M)*X3(M))/(CHORD*FVELOC*FVELOC)
      CMY=CLY*((XMY-XB1(1))*COS(FANGLE*PI/180.0)-(ZB1(1)-ZMY)*
     #SIN(FANGLE*PI/180.0))+CDY*((ZB1(1)-ZMY)*COS(FANGLE*PI/180.0)+
     #(XMY-XB1(1))*SIN(FANGLE*PI/180.0))
      WRITE(9,26)M,CLY,CDY,CMY
      CL=CL+CLY
      CD=CD+CDY
      CM=CM+CMY
   65 CONTINUE
      CL=CL/NSTRIP
      CD=CD/NSTRIP
      CM=CM/NSTRIP
      WRITE(9,27)CL,CD,CM
      DO 67 M=1,NSTRIP
      WRITE(9,28)M,VX2(M),VY2(M),VZ2(M)
   67 CONTINUE
C     ----------------------------------------------------------------
C     CALCULATION OF INDUCED VELOCITY AT THE FREE SURFACE CONTROL
C     POINTS DUE TO BODY AND IMAGE
C     N1=1 FOR BODY
C     N1=2 FOR IMAGE
C     ----------------------------------------------------------------
      DO 73 L=1,5
      DO 74 M=1,NSF
      X(M)=XF(M,L)
      Y(M)=YF(M,L)
      Z(M)=ZF(M,L)
      VXS(M,L)=0.0
      VYS(M,L)=0.0
      VZS(M,L)=0.0
      DO 75 N=1,NSTRIP
      X1(N)=XB1(N)
      Y1(N)=YB1(N)
      X2(N)=XB2(N)
      Y2(N)=YB2(N)
      DO 76 N1=1,2
      IF(N1.EQ.2)GO TO 77
```

```
      Z1(N)=ZB1(N)
      Z2(N)=ZB2(N)
      GO TO 78
 77   Z1(N)=2.0*(DEPTH+ZCI(N,2))-ZB1(N)
      Z2(N)=2.0*(DEPTH+ZCI(N+1,2))-ZB2(N)
 78   C(M,N)=((Y(M)-Y1(N))*(Z(M)-Z2(N)))-((Y(M)-Y2(N))*(Z(M)-Z1(N)))
      D(M,N)=((X(M)-X1(N))*(Z(M)-Z2(N)))-((X(M)-X2(N))*(Z(M)-Z1(N)))
      E(M,N)=((X(M)-X1(N))*(Y(M)-Y2(N)))-((X(M)-X2(N))*(Y(M)-Y1(N)))
      F(M,N)=(X2(N)-X1(N))*(X(M)-X1(N))+(Y2(N)-Y1(N))*(Y(M)-Y1(N))+
     #(Z2(N)-Z1(N))*(Z(M)-Z1(N))
      G(M,N)=(X2(N)-X1(N))*(X(M)-X2(N))+(Y2(N)-Y1(N))*(Y(M)-Y2(N))+
     #(Z2(N)-Z1(N))*(Z(M)-Z2(N))
      H(M,N)=SQRT((X(M)-X1(N))**2+(Y(M)-Y1(N))**2+(Z(M)-Z1(N))**2)
      P(M,N)=SQRT((X(M)-X2(N))**2+(Y(M)-Y2(N))**2+(Z(M)-Z2(N))**2)
      Q(M,N)=(Z(M)-Z1(N))**2+(Y1(N)-Y(M))**2
      R(M,N)=(Z(M)-Z2(N))**2+(Y2(N)-Y(M))**2
      S(M,N)=(F(M,N)/H(M,N))-(G(M,N)/P(M,N))
      T(M,N)=C(M,N)*C(M,N)+D(M,N)*D(M,N)+E(M,N)*E(M,N)
      CC(M,N)=((Z(M)-Z1(N))/Q(M,N))*(1.0+((X(M)-X1(N))/H(M,N)))-
     #((Z(M)-Z2(N))/R(M,N))*(1.0+((X(M)-X1(N))/P(M,N)))
      DD(M,N)=((Y1(N)-Y(M))/Q(M,N))*(1.0+((X(M)-X1(N))/H(M,N)))-
     #((Y2(N)-Y(M))/R(M,N))*(1.0+((X(M)-X2(N))/P(M,N)))
      U(M,N)=(C(M,N)*S(M,N)/T(M,N))/(4.0*PI)
      V(M,N)=(CC(M,N)-((D(M,N)*S(M,N))/T(M,N)))/(4.0*PI)
      W(M,N)=((E(M,N)*S(M,N)/T(M,N))+DD(M,N))/(4.0*PI)
      VXS(M,L)=VXS(M,L)+X3(N)*U(M,N)
      VYS(M,L)=VYS(M,L)+X3(N)*V(M,N)
      VZS(M,L)=VZS(M,L)+X3(N)*W(M,N)
  76  CONTINUE
  75  CONTINUE
  74  CONTINUE
  73  CONTINUE
C     ----------------------------------------------------------------
C     FREE SURFACE DEFLECTION AND SHAPE CALCULATION
C     ----------------------------------------------------------------
      DO 82 M=1,NSF
      ZCIL(M)=ZCI(M,2)
      DO 83 L=1,5
      ZCI(M,L)=-(FVELOC*VXS(M,L)+0.5*(VXS(M,L)*VXS(M,L)+
     #VYS(M,L)*VYS(M,L)+VZS(M,L)*VZS(M,L)))/9.81
      ZF(M,L)=DEPTH+ZCI(M,L)
      WRITE(9,32)M,L,VXS(M,L),VYS(M,L),VZS(M,L),ZCI(M,L),ZF(M,L)
  83  CONTINUE
  82  CONTINUE
C     ----------------------------------------------------------------
C     TEST FOR CONVERGENCE OF IMAGE DEFLECTION
C     ----------------------------------------------------------------
      IF(IZ.EQ.1)GO TO 55
      WRITE(9,41)IZ
      DO 84 M=1,NSF
      DZCI(M)=ABS((ZCI(M,2)-ZCIL(M))/ZCIL(M))
      WRITE(9,35)ZCIL(M),ZCI(M,2),DZCI(M)
  84  CONTINUE
      DO 85 M=1,NSF
      IF(DZCI(M).GT.0.001) GO TO 85
```

```
 85   CONTINUE
      WRITE(9,42)IZ
      GOTO 87
 86   IF(IZ.NE.MITER) WRITE(9,39)IZ
      IF(IZ.EQ.MITER) WRITE(9,40)IZ
 55   CONTINUE
 10   FORMAT(2F10.5)
 11   FORMAT(I2)
 12   FORMAT(9F7.4)
 13   FORMAT(5F10.5)
 14   FORMAT(50X,'DATA'/45X,14('-')/45X,14('-')///)
 15   FORMAT(//5X,'CHORD=',F10.5//5X,'SPAN=',F10.5)
 16   FORMAT(//5X,'NUMBER OF STRIP=',I3)
 17   FORMAT(////1X,'STRIP NO',10X,'X',11X,'Y',11X,'Z',10X,'X1',10X,
     #'Y1',10X,'Z1',10X,'X2',10X,'Y2',10X,'Z2'/1X,9('-'),6X,7('-'),5X,
     #7('-'),5X,7('-'),6X,6('-'),6X,6('-'),6X,6('-'),6X,6('-'),6X,
     #6('-'),6X,6('-'))
 18   FORMAT(//(3X,I3,9X,9(F9.5,3X)/))
 19   FORMAT(//5X,'SPEED OF FLOW=',F10.5//5X,'ANGLE OF ATTACK=',F10.5,
     #//5X,'DIHEDRAL ANGLE=',F10.5//5X,'SLOPE OF MEAN CAMBER LINE AT TH
     #E CONTROL POINT=',F10.5//5X,'DEPTH OF SUBMERGENCE=',F10.5)
 20   FORMAT(50X,'RESULT'/45X,16('-')/45X,16('-'))
 21   FORMAT(////(1X,10(E12.5,1X)/))
 22   FORMAT(/////(2X,10(E11.6,1X)))
 23   FORMAT(//5X,'STRIP NO.',10X,'CIRCULATION')
 24   FORMAT(/8X,I2,12X,E13.6)
 25   FORMAT(22X,'CLY',15X,'CDY',15X,'CMY'/18X,10('-'),8X,10('-'),9X,
     #10('-'))
 26   FORMAT(//4X,'M=',I5,5X,3(E13.6,5X))
 27   FORMAT(//5X,'CL=',E13.6//5X,'CD=',E13.6//5X,'CM=',E13.6)
 28   FORMAT(//(10X,'M=',I5,5X,'VX2=',E13.6,5X,'VY2=',E13.6,5X,
     #'VZ2=',E13.6))
 29   FORMAT(5X,'XF='/1X,10('-')//1X,5(E13.6,3X))
 30   FORMAT(5X,'YF='/1X,10('-')//1X,5(E13.6,3X))
 31   FORMAT(5X,'ZF='/1X,10('-')//1X,5(E13.6,3X))
 32   FORMAT(//(5X,'M=',I2,4X,'L=',I2,4X,'VXS=',E13.6,5X,'VYS=',
     #E13.6,5X,'VZS=',E13.6,5X,'ZETA=',E13.6,5X,'ZF=',E16.9))
 33   FORMAT(2F10.5)
 34   FORMAT(/5X,'X-ORDINATE OF MOMENT AXIS=',G10.4/5X,
     #'Y-ORDINATE OF MOMENT AXIS=',G10.4)
 35   FORMAT(5X,3E13.6)
 36   FORMAT(/5X,'CALCULATION STARTS FOR ITERATION NO.=',I5//)
 37   FORMAT(I2)
 38   FORMAT(/5X,'MAXIMUM NO. OF ITERATIONS REQUIRED=',I2)
 39   FORMAT(/5X,'SOLUTION IS NOT CONVERGED AFTER',3X,I2,7X,
     #'CONTINUE NEXT ITERATION')
 40   FORMAT(/5X,'SOLUTION IS NOT CONVERGED AFTER GIVEN MAXIMUM',
     #5X,I2,'ITERATIONS')
 41   FORMAT(/5X,'CONVERGENCE TEST AFTER',5X,I2,2X,'ITERATIONS')
 42   FORMAT(/5X,'SOLUTION IS CONVERGED AFTER',5X,I2,2X,'ITERATIONS')
 87   STOP
      END
C     |-----------------------------------------------------------------
C     |
C     |                 SUBROUTINE    SOLVE
```

```
      |
      |----------------------------------------------------------------

      SUBROUTINE SOLVE(A,B,M,X3)
      DIMENSION A(15,15),B(15),X3(15)
      MM=M-1
      DO 107 K=1,MM
      KP=K+1
      L=K
      DO 102 I=KP,M
      IF(ABS(A(I,K)).LE.ABS(A(L,K))) GO TO 102
      L=I
  102 CONTINUE
      IF(L-K)105,105,103
  103 DO 104 J=K,M
      AJ=A(K,J)
      A(K,J)=A(L,J)
  104 A(L,J)=AJ
      AB=B(K)
      B(K)=B(L)
      B(L)=AB

      ELEMINATION PROCESS

  105 DO 107 I=KP,M
      FAC=A(I,K)/A(K,K)
      A(I,K)=0.0
      DO 106 J=KP,M
  106 A(I,J)=A(I,J)-FAC*A(K,J)
  107 B(I)=B(I)-FAC*B(K)

      SOLUTION & BACK SUBSTITUTION

      X3(M)=B(M)/A(M,M)
      I=M-1
  108 I2=I+1
      SUM=0.0
      DO 109 J=I2,M
  109 SUM=SUM+A(I,J)*X3(J)
      X3(I)=(B(I)-SUM)/A(I,I)
      I=I-1
      IF(I)110,110,108
  110 RETURN
      END
```

APPENDIX-B

HYDROFOIL DATA

Table : Section Profile data of NACA 4412.

Station X (% of chord)	Z ordinate (% of chord)		
	Upper surface	Lower surface	Mean Surface
0	0	0	0
1.25	2.44	-1.43	1.935
2.5	3.39	-1.95	2.67
5.0	4.73	-2.49	3.61
7.5	5.76	-2.74	4.25
10.0	6.59	-2.86	4.725
15.0	7.89	-2.88	5.385
20.0	8.80	-2.74	5.77
30.0	9.76	-2.26	6.01
40.0	9.80	-1.80	5.80
50.0	9.19	-1.40	5.295
60.0	8.14	-1.00	5.57
70.0	6.69	-0.65	3.67
80.0	4.89	-0.39	2.64
90.0	2.71	-0.22	1.465
95.0	1.47	-0.16	0.815
100.0	0.13	-0.13	0.13

Table : Section profile data of NACA 16-206.

Station X(% of chord)	Z-ordinate (% of chord)		
	Upper surface	Lower surface	Mean surface
0	0	0	0
1.25	0.753	-0.539	0.646
2.5	1.089	-0.717	0.903
5.0	1.571	-0.939	1.255
7.5	1.940	-1.092	1.516
10.0	2.246	-1.212	1.726
15.0	2.740	-1.394	2.067
20.0	3.128	-1.536	2.332
30.0	3.681	-1.737	2.709
40.0	3.998	-1.856	2.927
50.0	4.103	-1.897	3.00
60.0	3.988	-1.846	2.917
70.0	3.607	-1.663	2.635
80.0	2.895	-1.303	2.099
90.0	1.776	-0.742	1.256
95.0	1.023	-0.391	0.707
100.0	0.060	-0.060	0

APPENDIX-C

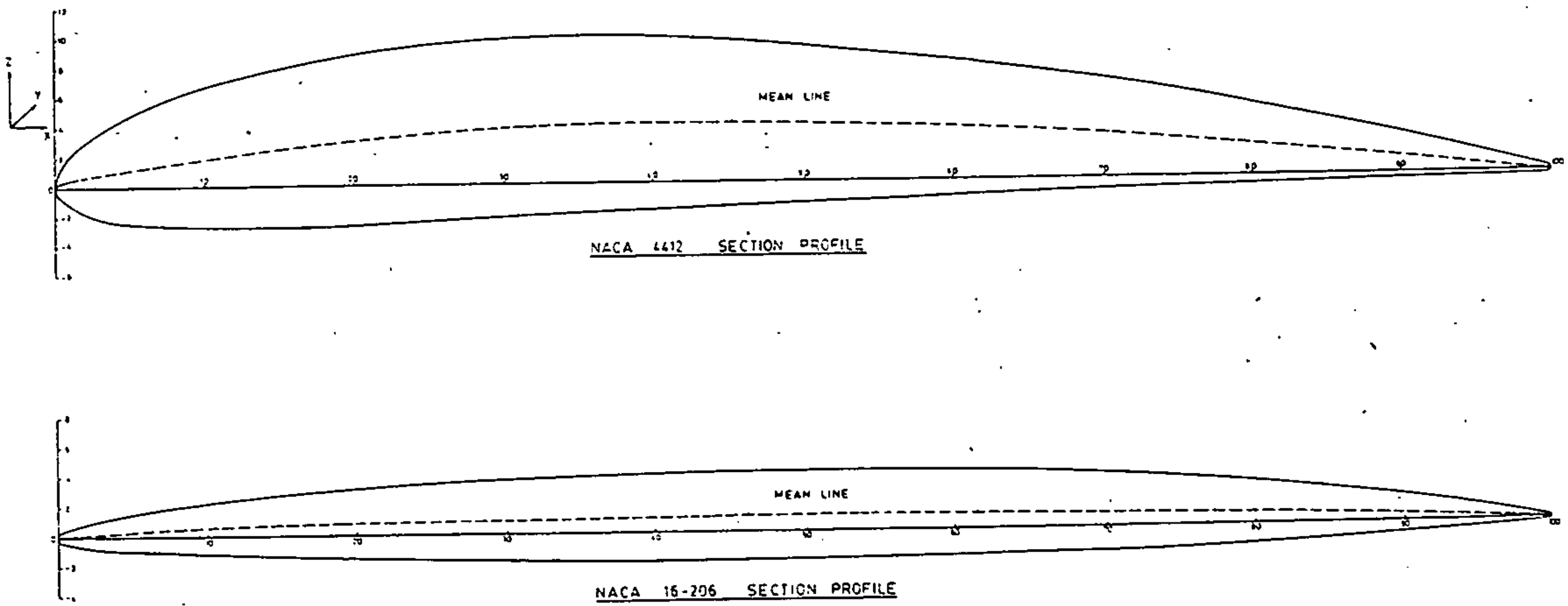

FIG. : SECTION PROFILE.

APPENDIX-D

Table : Variation of CPU time in second with number of iterations completed.

No.of itertion	CPU Time(sec)	
	Virtual	Total
2	14.49	19.12
3	18.76	23.31
4	24.81	30.82
5	30.06	36.65
6	35.72	43.68
7	39.83	46.81